

INVOLVEMENT OF NUCLEUS RAPHE MAGNUS IN NEURONAL EXCITABILITY OF LONG TERM PARACETAMOL-TREATED RATS



A Dissertation Submitted in Partial Fulfillment of the Requirements
for the Degree of Doctor of Philosophy in Physiology
Inter-Department of Physiology
Graduate School
Chulalongkorn University
Academic Year 2018
Copyright of Chulalongkorn University

ความเกี่ยวข้องของนิเวศวิทยส ราฟี่ แมกนัส ต่อการตื่นตัวของเซลล์ประสาทในหนูแรทที่ได้รับพาราเซตามอลเป็นเวลานาน



วิทยานิพนธ์นี้เป็นส่วนหนึ่งของการศึกษาตามหลักสูตรปริญญาวิทยาศาสตรดุษฎีบัณฑิต

สาขาวิชาสรีรวิทยา สหสาขาวิชาสรีรวิทยา

บัณฑิตวิทยาลัย จุฬาลงกรณ์มหาวิทยาลัย

ปีการศึกษา 2561

ลิขสิทธิ์ของจุฬาลงกรณ์มหาวิทยาลัย



จุฬาลงกรณ์มหาวิทยาลัย
CHULALONGKORN UNIVERSITY



จุฬาลงกรณ์มหาวิทยาลัย
CHULALONGKORN UNIVERSITY



จุฬาลงกรณ์มหาวิทยาลัย
CHULALONGKORN UNIVERSITY

ACKNOWLEDGEMENTS

I would like to express my sincere gratitude to my advisor, Asst. Prof. Weera Supronsinchai, for the continuous support of my Ph.D. study and research. His guidance helped me a lot both for the laboratory periods and the writing of this thesis. In addition, I would like to say thank you very much to my co-advisor, Prof. Anan Srikiatkachorn, for his patience, motivation and comments. He always inspires me to be a good faculty staff. Furthermore, I would like to give my sincere thanks to another co-advisor, Asst.Prof. Supang Maneesri le grand, for her encouragement, kindness and support in everything.

Besides I would like to thank the rest of my thesis committee, the faculty staffs from department of physiology in both medical and dental schools at Chulalongkorn university and my colleagues in the department of occlusion for the useful informations and mental support.

Furthermore, I am thankful to all my friends from the department of physiology, especially Miss Pornsiri Suwannaporn, for several guidances of laboratory technique, helps and supports. All your kindness will be stayed in my memory.

Finally, I would like to extend a huge thank you to my parents, sister and brother for all supporting in my life. I cannot be myself today without them.

จุฬาลงกรณ์มหาวิทยาลัย
CHULALONGKORN UNIVERSITY

Prangtip Potewiratnanond

TABLE OF CONTENTS

	Page
ABSTRACT (THAI)	iii
ABSTRACT (ENGLISH)	iv
ACKNOWLEDGEMENTS	v
TABLE OF CONTENTS	vi
FIGURE CONTENTS	ix
TABLE CONTENTS	xii
PAGE	xii
CHAPTER 1 INTRODUCTION.....	13
BACKGROUND AND RATIONALE	13
RESEARCH QUESTION.....	14
HYPOTHESIS.....	14
OBJECTIVES	14
CONCEPTUAL FRAMEWORK	15
KEYWORDS.....	15
CHAPTER 2 REVIEW OF LITERATURES.....	16
MEDICATION OVERUSE HEADACHE (MOH)	16
TRIGEMINAL NOCICEPTIVE SYSTEM.....	17
CENTRAL MODULATING SYSTEM AND NRM.....	20
ANIMAL MODELS OF MIGRAINE.....	21
FOS EXPRESSION.....	25
PARACETAMOL (ACETAMINOPHEN, APAP).....	26

CHAPTER 3 MATERIALS AND METHODS	29
RESEARCH DESIGN	29
RESEARCH METHODOLOGY	29
ANIMAL PREPARATION	31
CHEMICAL PREPARATION	32
ELECTROPHYSIOLOGICAL RECORDING.....	33
1) CORTICAL SPREADING DEPRESSION MODEL	33
a. SURGICAL PREPARATION.....	33
b. ELECTROCORTICOGRAPHIC RECORDING AND DATA COLLECTION.....	35
2) NTG-INDUCED HEADACHE MODEL	36
a. SURGICAL PREPARATION.....	36
b. EXTRACELLULAR RECORDING AT TNC AND DATA COLLECTION.....	36
IMMUNOHISTOCHEMICAL STUDY	37
1) PERFUSION AND TISSUE PREPARATION	37
2) IMMUNOHISTOCHEMICAL STAINING FOR THE FOS.....	38
3) DATA COLLECTION FOR THE IMMUNOREACTIVE CELLS.....	40
DATA ANALYSIS.....	41
CHAPTER 4 RESULTS	42
MICROINJECTION AREA.....	42
ELECTROCORTICOGRAPHIC RECORDING	43
CSD-EVOKED FOS EXPRESSION.....	46
MICROINJECTION AREA.....	59

EXTRACELLULAR RECORDING.....	60
CHAPTER 5 DISCUSSION AND CONCLUSION.....	73
EFFECT OF CHRONIC PARACETAMOL EXPOSURE.....	73
INVOLVEMENT OF NRM ON THE CORTICAL EXCITIBILITY	74
INVOLVEMENT OF NRM ON THE TRIGEMINAL NOCICEPTIVE SYSTEM	75
REFERENCES.....	77
VITA.....	87



FIGURE CONTENTS

	PAGE
Figure 1 Pathways of trigeminal nociceptive system	19
Figure 2 Nucleus raphe magnus	21
Figure 3 Possible actions of nitric oxide-induced headache	24
Figure 4 Paracetamol inhibits of the prostaglandins synthesis.....	27
Figure 5 Experimental design 1	30
Figure 6 Experimental design 2	31
Figure 7 The surgical areas for electrocorticographic recording.....	34
Figure 8 The surgical area for microinjection at nucleus raphe magnus	35
Figure 9 Example of spike latency of recording neurons.....	37
Figure 10 Fos staining protocol for paraffin-embedded sections of brain	39
Figure 11 Fos staining protocol for free-floating sections of trigeminal nucleus caudalis	40
Figure 12 Areas for data collection at cortex and trigeminal nucleus caudalis	41
Figure 13 Schematic of microinjected-site at nucleus raphe magnus in experiment 1	43
Figure 14 Effect of chronic paracetamol exposure on CSD development and modulating effect of microinjection into nucleus raphe magnus.	44
Figure 15 Effect of chronic paracetamol exposure on the number of CSD waves and modulating effect of microinjection into nucleus raphe magnus.	45
Figure 16 Photomicrograph shows the effect of CSD-evoked Fos expression in primary somatosensory cortex of control groups.....	48
Figure 17 Photomicrograph shows the effect of CSD-evoked Fos expression in primary somatosensory cortex of paracetamol-treated groups	49

Figure 18 Photomicrograph shows the effect of chronic paracetamol exposure and modulating effect of microninjection into nucleus raphe magnus on CSD-evoked Fos expression in primary somatosensory cortex.	50
Figure 19 Effects of chronic paracetamol exposure and modulating effect of microninjection into nucleus raphe magnus on CSD-evoked Fos expression in primary somatosensory cortex.....	52
Figure 20 Photomicrograph shows the effect of CSD-evoked Fos expression in trigeminal nucleus caudalis of control groups.	54
Figure 21 Photomicrograph shows the effect of CSD-evoked Fos expression in trigeminal nucleus caudalis of paracetamol-treated groups.	55
Figure 22 Photomicrograph shows the effects of chronic paracetamol exposure and modulating effect of microninjection into nucleus raphe magnus on CSD-evoked Fos expression in trigeminal nucleus caudalis.	56
Figure 23 Effects of chronic paracetamol exposure and modulating effect of microninjection into nucleus raphe magnus on CSD-evoked Fos expression in trigeminal nucleus caudalis.....	58
Figure 24 Schematic of microinjected-site at nucleus raphe magnus in experiment 2	59
Figure 25 Modulating effect of microinjection into nucleus raphe magnus on nitroglycerin-evoked neuronal firing in trigeminal nucleus caudalis (representative records of patterns of TNC firing).	60
Figure 26 Effect of chronic paracetamol exposure and modulating effect of microninjection into nucleus raphe magnus on nitroglycerin-evoked neuronal firing in trigeminal nucleus caudalis (representative records of patterns of TNC firing).....	61
Figure 27 Effect of chronic paracetamol exposure and modulating effect of microinjection into nucleus raphe magnus on nitroglycerin-evoked neuronal firing in trigeminal nucleus caudalis.	65

Figure 28 Photomicrograph shows the effects of chronic paracetamol exposure and modulating effect of microninjection into nucleus raphe magnus on nitroglycerin-evoked Fos expression at primary somatosensory cortex.	67
Figure 29 Effect of chronic paracetamol exposure and modulating effect of microninjection into nucleus raphe magnus on nitroglycerin-evoked Fos expression at primary somatosensory cortex.....	69
Figure 30 Photomicrograph shows the effects of chronic paracetamol exposure and modulating effect of microninjection into nucleus raphe magnus on nitroglycerin-evoked Fos expression at trigeminal nucleus caudalis.	71
Figure 31 Effects of chronic paracetamol exposure and modulating effect of microninjection into nucleus raphe magnus on nitroglycerin-evoked Fos expression at trigeminal nucleus caudalis.	72

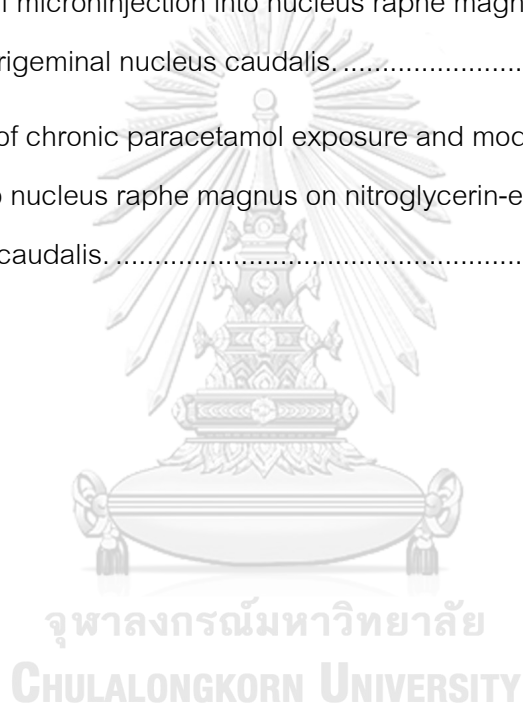


TABLE CONTENTS

	PAGE
Table 1 The average numbers of CSD wave after microinjection at nucleus raphe magnus area.....	46
Table 2 The average numbers of CSD-evoked Fos expression in cortical neuron of primary somatosensory cortex.....	51
Table 3 The average numbers of CSD-evoked Fos expression in neurons of trigeminal nucleus caudalis.....	57
Table 4 The average of neuronal firing at trigeminal nucleus caudalis after nitroglycerin infusion	62
Table 5 The average of neuronal firing at trigeminal nucleus caudalis after nucleus raphe magnus microinjection	63
Table 6 The average numbers of nitroglycerin-evoked Fos expression in cortical neurons of primary somatosensory cortex.....	68
Table 7 The average numbers of nitroglycerin-evoked Fos expression in neurons of trigeminal nucleus caudalis	72

CHAPTER 1

INTRODUCTION

BACKGROUND AND RATIONALE

Medication overuse headache (MOH) is one of the most common chronic headache disorders (1). It is found 1-2% in the world population (2). The prevalence of MOH is approximately half of patients with chronic headache. MOH develops after overuse of acute or symptomatic headache drugs in primary headache patients, especially migraineurs. The manifestation of MOH is described as an increased frequency of headache (15 or more days per month for more than 3 months) and also suffering from other clinical symptoms, such as depressed mood and sleep disturbance (1). From the epidemiological study, patients with MOH reports disability and poor quality of life. An understanding of MOH mechanism may provide the effective prevention and treatment.

Based on the previous studies, pathophysiology of MOH was reported as an alteration of trigeminal nociceptive system and an increase of the cortical excitability (3-6). Interestingly, Srikiatkhachorn A. and colleagues suggested the clues receiving from clinical observations in patients with MOH which may relate to the mechanisms of MOH (7). From the observations, they proposed that analgesic overuse is the cause of chronic headache and central nervous system plays an important role in the mechanism of MOH. In addition, all analgesics or specific-headache drugs seem to share a common mechanism in generating MOH. Moreover, an abnormality of the other neural systems is involved in the MOH condition. Finally, they hypothesized that chronic medication may alter the central modulating system leading to MOH in susceptible patients.

The central modulating system is mediated by several neurotransmitters in brainstem nuclei to optimize the central nervous system activity (8). Serotonin neurotransmitter, which has the main source in raphe nuclei, was shown to involve in the pathogenesis of MOH (9-11). Because of nucleus raphe magnus (NRM) is a

serotonergic brainstem nucleus, it is possible that chronic medication may affect NRM function.

Paracetamol is a non-specific analgesic drug of choice for mild to moderate headache. It is used worldwide for its cost-effectiveness and access availability. However, an overuse of paracetamol may induce MOH (1). The previous study demonstrated an increase in CSD evoked-neuronal excitability at cortex and trigeminal nucleus caudalis (TNC) in chronic paracetamol-administered rats (12). This study aimed to investigate an involvement of NRM in neuronal excitability of chronic paracetamol-treated rats.

RESEARCH QUESTION

Does a chronic paracetamol treatment increase the neuronal excitability in cortex and trigeminal nucleus caudalis via nucleus raphe magnus?

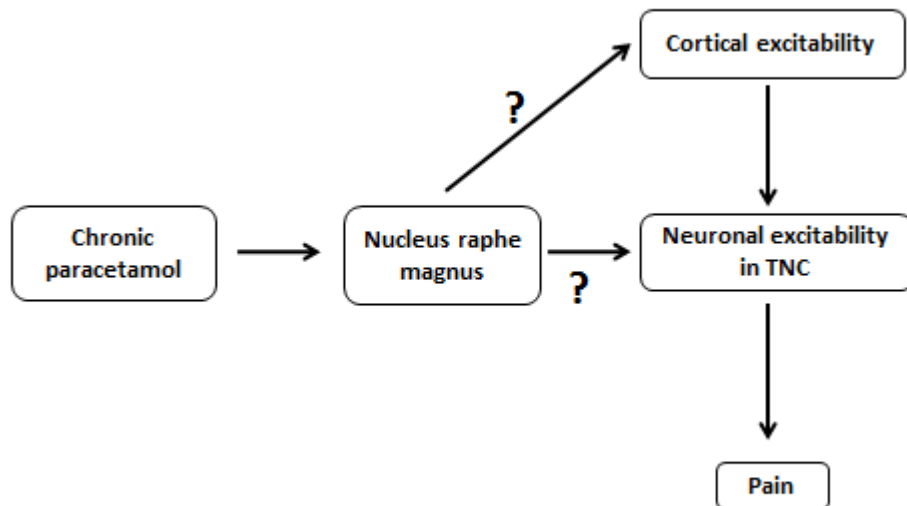
HYPOTHESIS

A chronic paracetamol treatment increases the neuronal excitability in cortex and trigeminal nucleus caudalis via nucleus raphe magnus.

OBJECTIVES

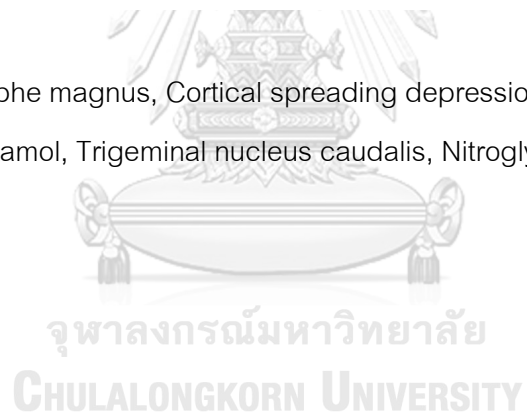
1. To examine an involvement of nucleus raphe magnus on cortical spreading depression-evoked neuronal excitability of chronic paracetamol-treated rats
2. To examine an involvement of nucleus raphe magnus on nitroglycerin-induced neuronal excitability of chronic paracetamol-treated rats

CONCEPTUAL FRAMEWORK



KEYWORDS

Nucleus raphe magnus, Cortical spreading depression, Medication overuse headache, Paracetamol, Trigeminal nucleus caudalis, Nitroglycerin



CHAPTER 2

REVIEW OF LITERATURES

MEDICATION OVERUSE HEADACHE (MOH)

Medication overuse headache (MOH) previously calls rebound headache, drug-induced headache or medication-misuse headache. MOH develops after overuse of acute or symptomatic drugs and mostly occurs in migraine and tension-type headache patients (1). The manifestation of MOH is described as an increased frequency of headache (15 or more days per month for more than 3 months) and also suffering from other clinical symptoms, such as depressed mood and sleep disturbance (1). It is important in clinical diagnosis because approximately half of people with headache on 15 or more days per month for more than 3 months have MOH (1). Although the mechanisms underlying pathogenesis of MOH remain unclear, there are numerous investigations which provided the interesting knowledge regarding pathogenesis of MOH.

Clinical evidences indicated that patients with MOH had an increase of neuronal activity at the supraspinal level (6, 13, 14). The hyperexcitability of neurons in this condition may a result from neurotransmitter changes, for example serotonin reduction. As Srikiatkachorn A. et al. reported that the platelet serotonin was decreased (15), while the density of 5HT_{2A} receptors on platelets was increased (16) and normalized after drug withdrawal (17) in patients with MOH. Consistently, chronic analgesic-administrated rats in several drug classes elicited neuroadaptive changes in trigeminal nociceptive system leading to neuronal hyperexcitability. For instance, Okada-Ogawa A. and colleagues reported that sustained-morphine exposure rats expanded cutaneous receptive field and reduced threshold stimuli (3). Additionally, an enhancement of calcitonin gene-related peptide (CGRP) expression in dorsal root ganglion culture cells and CGRP release from the primary afferent neurons in sustained-morphine exposure condition were demonstrated in studies from Ma J. et al. and Gardell L.R. et al., respectively (4, 18). CGRP is a neuropeptide which reported as a modulator of

nociceptive transmission (19). An elevation of CGRP seems to decrease the descending inhibitory pain mechanism and facilitate pain transmission (20). Furthermore, persistent-triptans administration to rats elicited cutaneous allodynia in periorbital area and hind paw. Allodynia is a clinical manifestation that represents a state of central sensitization (5). Also, long term dihydroergotamine or paracetamol exposure can increase Fos expression in the TNC and cortex of rats which indicated an enhancement of neuronal activity (12, 21).

An alteration of the descending pain control system has been reported in patients with MOH. Perrotta A. and colleagues demonstrated that MOH patients showed abnormality of pain transmission and loss of diffuse nociceptive inhibitory control (DNIC) (22). They studied an abnormality of descending pain control system by evaluating the effect of heterotopic nociceptive stimuli which activate the DNIC. Additionally, the anatomical studies from Riederer F. and colleagues using magnetic resonance imaging (MRI) demonstrated changes in gray matter volume of brainstem structures in patients with MOH (23, 24). In animal investigations, electrophysiological study from Meng I.D. and colleagues revealed that chronic morphine increased the proportion of on-cells, a group of cells which responds to noxious stimuli, in rostral ventromedial medulla (RVM) (25). Furthermore, Vanderah T.W. et al. reported that microinjection of lidocaine into the RVM caused the reversible blockade of sustain morphine-induced allodynia and hyperalgesia (26). Moreover, Okada-Ogawa A. et al. informed that sustained-morphine exposure eliminated DNIC in rats which can be reestablished after inactivation of the RVM (3). Loss of DNIC in sustained morphine-treated rats is consistent with the study from Perrotta A. et al. in MOH patients (22).

TRIGEMINAL NOCICEPTIVE SYSTEM

Trigeminal nerve is the principal sensory nerve of the head and face (27). Its three major branches, namely ophthalmic, maxillary and mandibular branches, are derived from the trigeminal ganglion (TG). The trigeminal innervations which relate to primary headache symptom mostly come from ophthalmic branch, including the fibers

surrounding the large cerebral vessels, pial vessels, large venous sinuses and dura mater (28).

Based on the anatomical studies, the main areas and groups of neurons related to the trigeminal pain transmission are described. The ascending trigeminal pain transmission is demonstrated in Figure 1. When pain is initiated, the nociceptive inputs are transferred through the first, second and third order neurons respectively, before signal translation in brain. Trigeminal afferent fibers can be categorized into three main groups which are A_{β} , A_{δ} and C-fibers (27). The small diameter nerve fibers, A_{δ} and C-fibers, were shown to convey pain sensation run from neurons in the trigeminal ganglion through the pons and medulla. These primary afferent fibers involve in the spinal trigeminal tract and terminate in the trigeminal spinal nucleus. Trigeminal spinal nucleus can be subdivided into trigeminal nucleus oralis, trigeminal nucleus interpolaris and trigeminal nucleus caudalis (TNC) which is known as the principal brainstem relay site for nociceptive information from the head and face (27, 29). Additionally, the primary afferent fibers are found predominantly in the superficial (I/II) and deep (V/VI) lamina of TNC (30). The second order neurons in TNC decussate and terminate in the contralateral ventral posteromedial nucleus (VPM) of the thalamus and brainstem areas, whereas the third order neurons from VPM of the thalamus project to the face area of the somatosensory cortex on the inferior portion of the postcentral gyrus where initial cortical processing takes place.

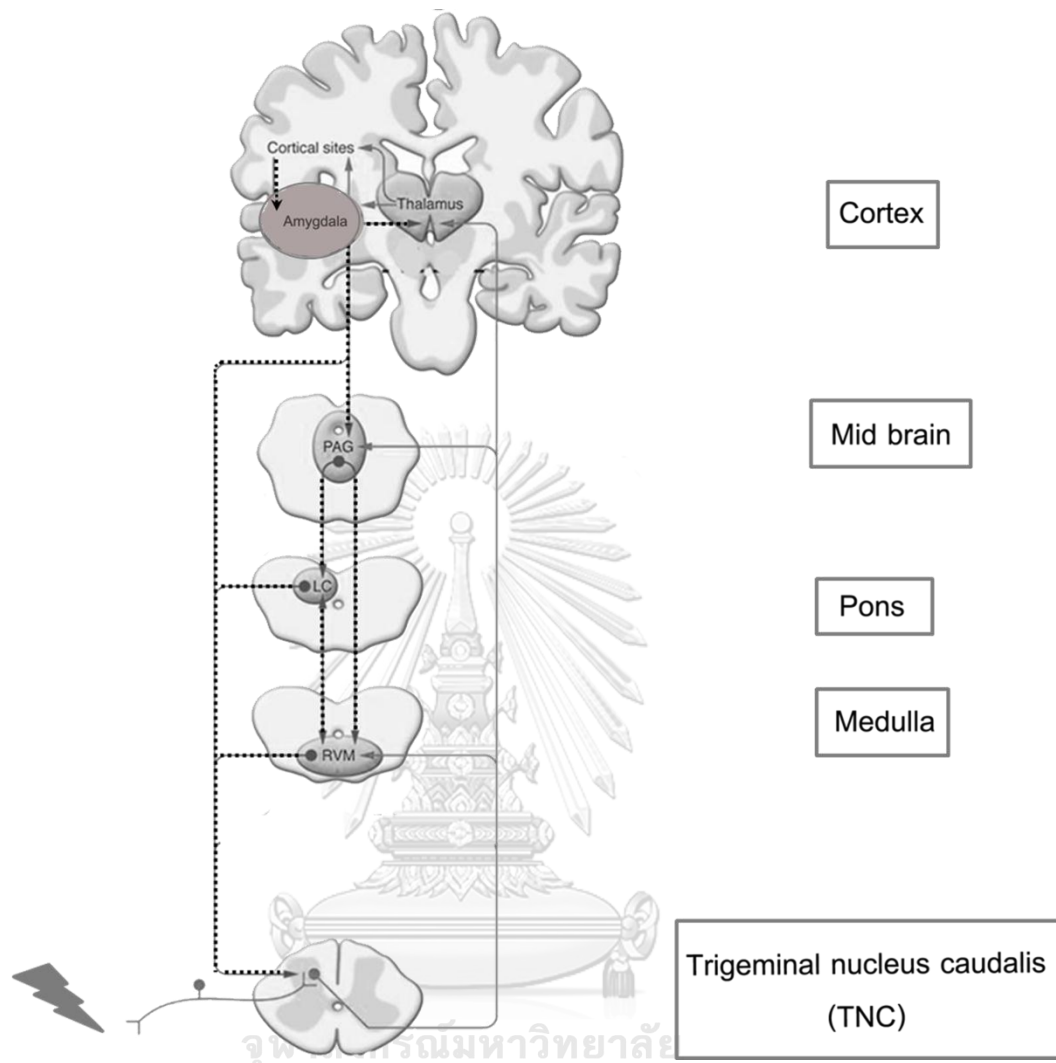


Figure 1 Pathways of trigeminal nociceptive system

Trigeminal afferent fibers convey nociceptive inputs through the neurons in trigeminal nucleus caudalis which their fibers decussate and terminate in the thalamus. The signals from thalamus were sent to the somatosensory cortex where perceptions of pain are integrated. Additionally, pain transmission is mediated by brainstem nuclei, especially PAG, LC, RVM. These nuclei send descending projection to modulate nociceptive transmission at medullary dorsal horn neurons of trigeminal nucleus caudalis. Figure was adapted from Ossipov MH. (30). LC, locus coeruleus; PAG, periaqueductal grey; RVM, rostral ventromedial medulla.

Mechanisms of trigeminal pain processing also contain the descending pain control projections to modulate the nociceptive inputs (Figure 1). This is a top-down pathway which mainly controls by neurons in brainstem (31). Focusing on the pathophysiology of the primary headache, especially migraine, the main structures for descending modulation are hypothalamus, periaqueductal grey (PAG), locus coeruleus (LC) and NRM, the major nucleus in RVM (28).

CENTRAL MODULATING SYSTEM AND NRM

The central modulating system is mediated by several brainstem nuclei which provide ascending projections to brain and descending projections to spinal cord. Its function contributes to optimize the central nervous system activity by using several neurotransmitters, including acetylcholine, norepinephrine, epinephrine, dopamine, histamine and serotonin (8). For example, these cholinergic and monoaminergic neurons are shown to regulate the internal homeostasis, pain perception and behavioral arousal (8). An involvement of central modulating system in the pathogenesis of MOH was hypothesized by Srikiatkachorn and colleagues based on the evidences from clinical observations. They reported that patients with MOH also suffer from the problem of vegetative functions which regulate by central modulating system, such as depressed mood and sleep disturbance (7). Additionally, an alteration of serotonergic receptor was found in patients with MOH (17). Preclinical study also supports clinical findings, a combination of the overuse of rizatriptan, specific migraine drug, and stimulation with dural inflammatory soup led to decrease of serotonin expression and upregulation of 5-HT_{2A} receptors (11)

NRM is a part of raphe nuclei which is a serotonergic brainstem nucleus. It is located in the caudal pons and the most rostral portion of the medulla at the midline (32) (Figure 2). Anatomical studies of NRM have shown that most of the 5-HT neurons project to the spinal cord, while very few 5-HT containing neurons and non 5-HT neurons form a significant ascending projection through the median forebrain bundle (MFB) (33). NRM was shown to involve in the generation of migraine headache through cortico-NRM-trigeminal nucleus neuraxis (34). This study demonstrated that neuronal activation

of the cortex can decrease the neuronal activity of the NRM in responses of trigeminal neurons. Besides, NRM was shown to play an important role in the spinal modulatory pain transmission by descending inhibitory influence (31). However, substantial evidences showed biphasic pain modulation (facilitation or inhibition) of NRM (35). This may a result from several neurotransmitters and neuropeptides contained in NRM neurons. Not only serotonergic neurons but also glycinergic, GABAergic and opiodergic neurons were found in NRM (36).

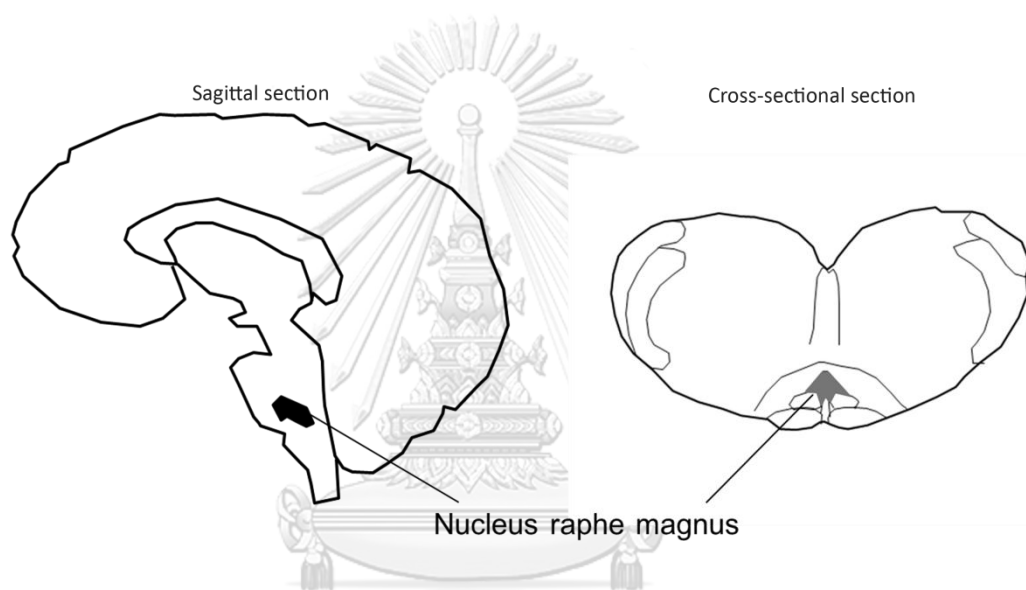


Figure 2 Nucleus raphe magnus

ANIMAL MODELS OF MIGRAINE

The animal models of migraine have been developed based on an understanding of migraine pathogenesis from humans. These models can be divided into two main categories regarding to the pathophysiology of migraine which are models of the headache phase and models of the other migraine symptoms, such as aura.

Models of the activation of trigeminovascular system

The method commonly reproduced the headache phase are the activation of trigeminovascular system regarding to the concept that migraine pain involves the sole sensory trigeminal innervation of the cerebral vessels, especially at dural and facial

structures (37). Electrical, mechanical and chemical stimulation are common methods of inducing activation in this system, e.g. passed square wave electrical pulse on dural vessels, repeated von Frey filaments testing on dural structures and applied inflammatory mediators on meninges. However, there are some limitations which should be concern in each stimulating method. For instance, electrical stimulation is not a physiological stimulus (38). It is only model which develop to approach painful nature. Additionally, topical application of inflammatory mediators to the dura could alter blood-brain-barrier functioning which directly activate central mechanism rather than stimulate peripheral afferent fibers (38).

Nitroglycerin (NTG) was demonstrated to induce headache immediately during the infusion and lead to a typical migraine attack one to several hours after termination of the infusion in migraineurs and healthy volunteers (39, 40). The evidences have been shown that nitric oxide (NO) donating from NTG is the key molecule for initiating headache in human (40, 41). Futhermore, NO-induced migraine was demonstrated to act on peripheral site (42, 43). The observations in human lead to a using of NO donors as a headache stimulant in animal study. Though, dosage of NO donors which commonly infused in animals was higher than those required to initiate headache in humans (38). Nowadays, NTG infusion is proposed as a valid model for episodic and chronic migraine headache in animal (44, 45). Three main reasons were described to support this idea. Firstly, NO donors can induce headache and premonitory symptoms similar to migraine (40, 42). In addition, these migraine symptoms can be aborted by nitric oxide synthase (NOS) inhibition (46). Secondly, NO donor was shown to activate the trigeminovascular system (47, 48). Finally, specific antimigraine drug, such as sumatriptan, was reported to reduce NTG- induced pain response (43, 45).

The effects of NO-induced headache possibly associate to cerebrovascular dilation and neuromodulating function in the trigeminal nociceptive system through NO-cyclic guanosine monophosphate (cGMP) pathway (49). The studies from Kruuse C. and colleagues (2002, 2003) supported that the main mechanism of NO-induced headache involved in NO-cGMP pathway (50, 51). These studies were demonstrated

that sildenafil, a selective inhibitor of cGMP-hydrolyzing phosphodiesterase 5, can induce more headache than placebo in normal subjects and migraineurs. The NO-cGMP pathway was shown in Figure 3. In brief, NO activates the enzyme-soluble guanylate cyclase. Then, this enzyme stimulates the production of cGMP. After that, this second messenger cGMP phosphorylates protein kinase G which has many intracellular functions. In the vascular smooth muscle cells, phosphorylation of protein kinase G results in an opening of calcium-activated potassium channels (52). This pathway leads to a vasodilation. Additionally, changes in gene expression from NO-cGMP pathway may occur in neurons leading to an alteration of the cell response to variety of stimuli. Reuter U. et al. (2001) reported that delayed dose-dependent inducible nitric oxide synthase (iNOS) mRNA upregulated in dura mater at second hour and increased corresponding protein expression at fourth, sixth and tenth hour after NTG infusion (53). Besides, other actions of NO may associate to NO-induced headache. For instance, NO was shown to facilitate the release of CGRP, the key factor of migraine initiation, by activating of voltage gated Ca^{2+} channel (54). Consequently, CGRP was shown to induce vasodilation and delayed migraine headache (55). Also, Ferrari L.F. et al. (2016) reported that the delayed-onset mechanical hyperalgesia induced by intradermal NTG is mediated by an activation of mast cells (56). They suggested that the endothelial cells were stimulated by the mediators from mast cells and release adenosine triphosphate (ATP) to act on P2X3 purinergic receptor, a ligand-gated ion channel, in perivascular nociceptors.

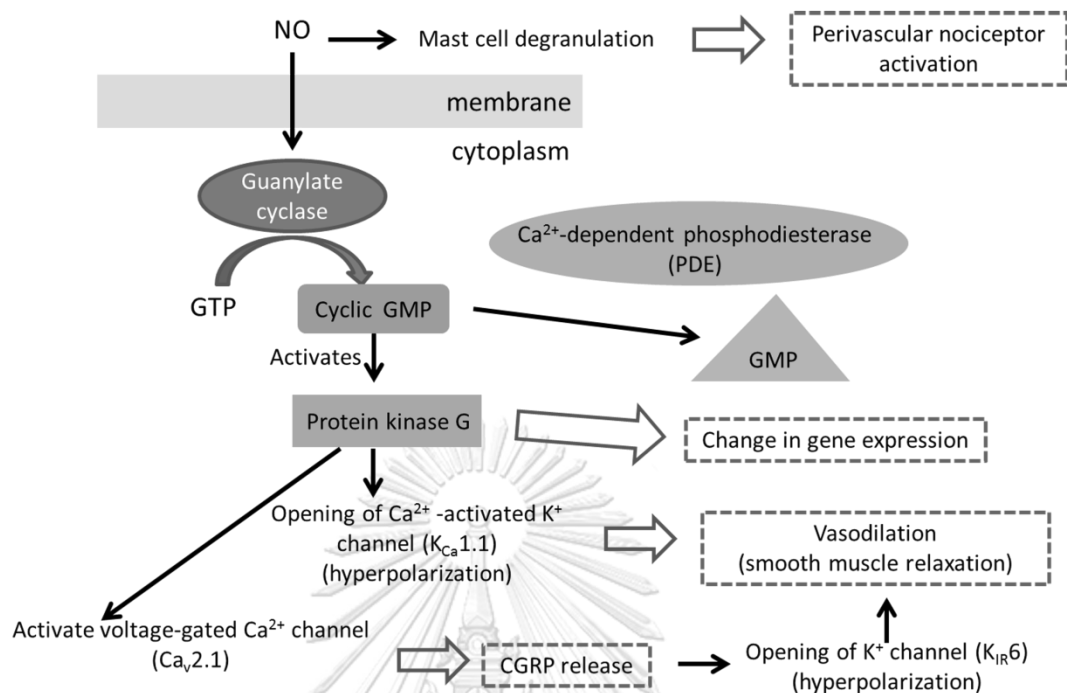


Figure 3 Possible actions of nitric oxide-induced headache

NO activates the enzyme-soluble guanylate cyclase. This enzyme stimulates the production of cGMP. After that, this second messenger cGMP phosphorylates protein kinase G which has many intracellular functions. For instance, the ability to control the function of ion channels results in vasodilation and release of CGRP. In addition, protein kinase G-induced changes in gene expression may occur in neurons leading to an alteration of the cell response to variety of stimuli. Moreover, an activation of mast cells from NO was shown to activate perivascular nociceptor. CGRP, calcitonin gene-related peptide; NO, nitric oxide; cGMP, cyclic guanosine monophosphate; cGTP, cyclic guanosine triphosphate.

Models of cortical spreading depression (CSD)

Cortical spreading depression (CSD) is known as a fundamental mechanism of migraine aura which refer to transient focal neurological deficits, such as visual impairment (57). CSD was shown to facilitate a synaptic transmission leading to excitability in the cortex (58). Furthermore, CSD event was reported as a noxious

stimulus to trigeminovascular system at the first and second order neurons (59, 60). In animal models, CSD induction is widely used as a migraine model which represents the cortical excitability condition.

CSD is a phenomenon firstly described by Leao A.A.P. in 1944 (61). The characteristics of CSD involve a slowly propagated wave of neuronal and glial membrane depolarization, followed by a sustained suppression of spontaneous neuronal activity, changes in vascular calibre, blood flow and energy metabolism (57, 61). CSD wave propagation results from a massive potassium ion (K^+) efflux which is believed to depolarize adjacent cells, exacerbated by glutamate release and calcium ion (Ca^{2+}) influx (62). An increase of intracellular Ca^{2+} and extracellular H^+ , K^+ , glutamate, arachidonic acid and nitric oxide are able to activate trigeminovascular system. In animal models, electrical, mechanical or chemical stimulation which affect the release of ions or the neurotransmitters, for example K^+ , Ca^{2+} and glutamate, can induce CSD propagation. CSD can be measured by electrocorticographic recording of direct current (DC) shift. Also, imaging studies, including MRI and optical intrinsic signal imaging are used for CSD measurement. The alteration of the CSD variables, such as the number of CSD wave, seems to represent the changes of neuronal sensitization.

In a potential connection between CSD and MOH, Chronic triptans exposure, migraine specific agent, significantly decreased electrical stimulation threshold to generate a CSD event in rats (63). Consistently, 30-days paracetamol administered rats showed an increase in the number of CSD wave (12). Moreover, a significant increase of area under the curve from the CSD amplitude in 30 days dihydroergotamine-treated rats was reported (21). All these previous studies were reported an alteration of CSD event which associate to a cortical hyperexcitability in long term drug-exposed animals.

FOS EXPRESSION

The c-fos is a proto-oncogene that is expressed within some neurons after changing the open time of voltage-gated calcium channels (64). Neuronal excitation leads to a rapid and transient induction of c-fos by increasing calcium ions influx (64).

The c-fos protein or Fos is the product of the c-fos gene which regulates the transcription of other target genes (44). At least three second-messenger systems are coupled to Fos induction i.e. protein kinase C, cAMP, calcium-calmodulin (44). This nuclear protein can be detected within the nuclei of neuron by immunohistochemical technique 20-90 minutes after neuronal excitation and disappears 4-16 hours later (65).

The expression of Fos widely used as a transynaptic marker for neuronal activity following noxious stimulation at a single cell level because the basal expression of Fos is very low and high-threshold noxious stimuli can induce a very dramatic increase of Fos expression (66, 67). Additionally, the pattern of Fos expression is topographically correlated with primary afferent projection (67). In trigeminal nociceptive system, TNC, brainstem, thalamus and cortex are widely chosen to detect Fos expression. However, Fos protein cannot be expressed in some structures, such as trigeminal ganglion (TG).

Since Fos expression is specific, easy to perform and quantify, it is broadly used as a marker for neuronal activation after long-term analgesic treatments in animals. Concerning migraine-specific agents, Green and colleagues reported that sumatriptan pre-exposure for 7 days significantly decreased CSD thresholds and increased Fos expression in the TNC (63). Furthermore, chronic rizatriptan exposure was reported to obviously increased the number of Fos immune-reactive cells in TNC (11). Consistently, chronic paracetamol and dihydroergotamine administration enhanced CSD-evoked Fos expression in cortex and TNC (12, 21). All these studies indicate an increase in cortical excitability and facilitation of trigeminal nociceptive system.

PARACETAMOL (ACETAMINOPHEN, APAP)

Paracetamol is an analgesic, antipyretic and weak anti-inflammatory drug. It is worldwide used to reduce mild to moderate pain and fever. Although an action of paracetamol was shown in both central and peripheral sites, its action appears to be mostly central. An analgesic effect of paracetamol mainly relates to inhibition of prostaglandin (PG) synthesis from arachidonic acid. The other effect is related to the

change in neural system, including serotonergic system and cannabinoid receptor activity.

Paracetamol is reported to reduce the active form of prostaglandin-endoperoxide synthase (PTGS) enzyme in PG synthesis. Normally, the conversion of arachidonic acid to prostaglandin occurs at two different site of PTGS enzyme, cyclooxygenase (COX) and peroxidase (POX) sites. The tyrosine-385 radical (Tyr385*) at the COX site transforms arachidonic acid to PGG₂ (68). Then, PGG₂ is reduced to PGH₂ by a ferryl protoporphyrin IX radical cation (Fe⁴⁺=OPP*⁺) at the POX site (69). Paracetamol was shown to reduce Fe⁴⁺=OPP*⁺ (70). Therefore, PG synthesis was inhibited. (Figure 4)

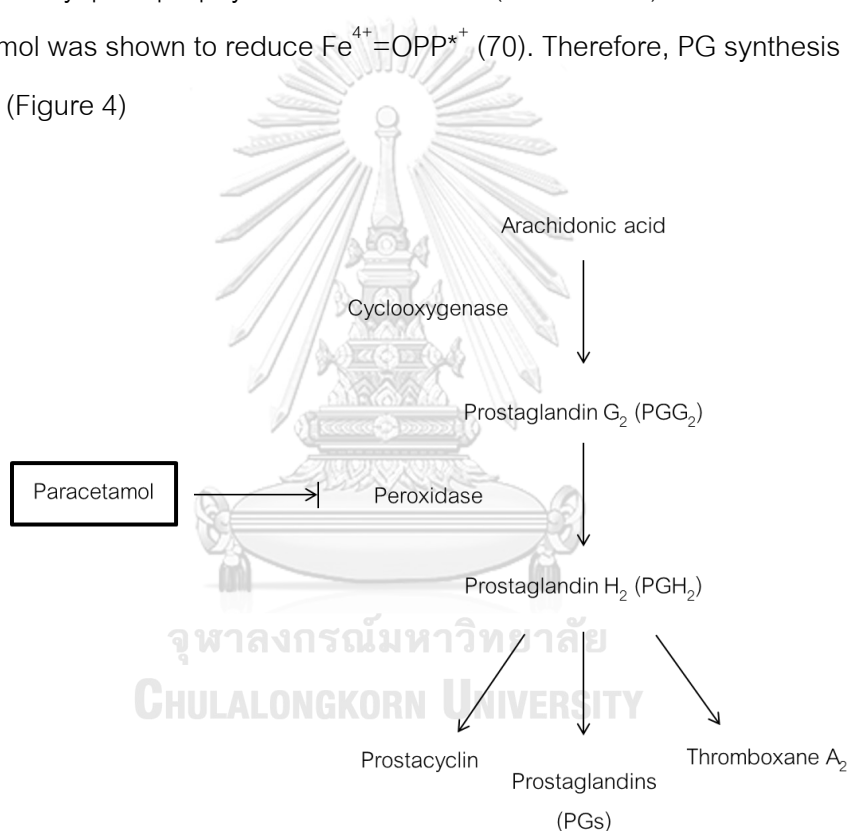


Figure 4 Paracetamol inhibits of the prostaglandins synthesis

Paracetamol was shown to inhibit prostaglandins synthesis at the peroxidase site of prostaglandin-endoperoxide synthase enzyme.

There are several studies reported that serotonergic and endogenous cannabinoids system are associated the antinociceptive action of paracetamol. For example, in human studies, the co-administration of 5-HT₃ receptor antagonists with

paracetamol changed the analgesic action produced by paracetamol (71, 72). Tjolsen and colleagues (1991) demonstrated that the analgesic action from paracetamol in formalin test was reduced after serotonin pathway was lesioned with intrathecal 5,6-dihydrotryptamine (5,6-DHT) (73). Additionally, Sandrini M. et al. (74) reported the 5-HT₂ receptor number at the prefrontal cortex decreased after paracetamol administration. Alternatively, an active metabolite of paracetamol, the fatty acid amide N-arachidonoylphenolamine (AM404), was demonstrated to inhibit endocannabinoid uptake leading to pain reduction by cannabinoid receptor activation (75).

Although there are several studies about paracetamol actions, the study of long-term effect to the neural system still requires. Recent studies from Blecharz and colleagues (76, 77) reported that serotonin was increased in the prefrontal cortex and medulla oblongata after chronic paracetamol treatment. In addition, long term paracetamol-treated rats also increased 5-HT_{2A} receptor at the trigeminal ganglion and cortex (10).

The major adverse effect of paracetamol is hepatotoxicity. It is usually due to an overconsumption of paracetamol leading to an imbalance of the paracetamol toxic metabolites and its reaction with glutathione. In general, paracetamol toxic metabolite, N-acetyl-p-benzouinoneimine (NAPQI), can be neutralized by glutathione and eliminated in urine and bile (78). However, an excessive paracetamol result in greater NAPQI formation. After glutathione is exhausted, un-neutralized NAPQI is free react with alternative targets leading to cell necrosis in the liver (79).

CHAPTER 3

MATERIALS AND METHODS

RESEARCH DESIGN

Laboratory experimental research

RESEARCH METHODOLOGY

EXPERIMENTAL DESIGN 1: To examine an involvement of NRM on cortical excitability and neuronal excitability in TNC of chronic paracetamol-treated rats after activated by KCl crystal (Figure 5)

- 1) Male Wistar rats were separated into two main groups, paracetamol-treated and control groups. The rats in paracetamol-treated group were intraperitoneally injected with 200 mg/kg paracetamol for 30 days while the rats in control group were injected with 0.9% NaCl.
- 2) On day 31st, electrocorticographic signaling was continuously recorded for 2 hours after CSD initiation. In addition, rats in control and paracetamol-treated groups were microinjected at NRM with 0.2 μ l glutamate, muscimol or 0.9% NaCl 30 minutes later after CSD initiation.
- 3) After electrocorticographic recording for 2 hours, rats were euthanized with sodium pentobarbital and prepared for immunohistochemical staining. The microinjected-site was assessed by checking histological sections with a light microscope. Only rats showing dyes spot in the NRM were considered for analysis.

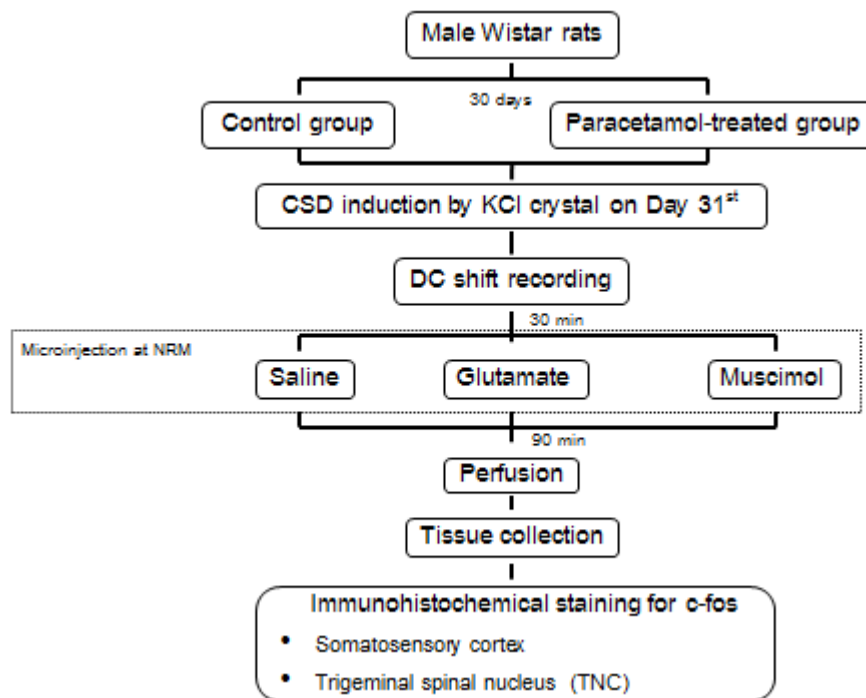


Figure 5 Experimental design 1

To examine an involvement of NRM on cortical excitability and neuronal excitability in TNC of chronic paracetamol-treated rats after activated by KCl crystal.

EXPERIMENTAL DESIGN 2: To examine an involvement of NRM on neuronal excitability in TNC of chronic paracetamol-treated rats after activated by NTG (Figure 6)

- 1) Male Wistar rats were separated into two main groups, paracetamol-treated and control groups. The rats in paracetamol-treated group were intraperitoneally injected with 200 mg/kg paracetamol for 30 days while the rats in control group were injected with 0.9% NaCl.
- 2) On day 31st, the neurons in TNC were identified by mechanical and electrical stimulation before extracellular recording. Spontaneous neuronal activity was recorded for 10 minutes as baseline. Then, NTG was continuously infused into the femoral vein to induce neuronal excitability for 2 hours. One hour after NTG infusion, the rats in control and paracetamol-treated group were microinjected

with 0.2 μ l glutamate, muscimol or 0.9% NaCl at NRM. The extracellular recording was finished 1 hour after microinjection.

- 3) After finished extracellular recording, the rats were euthanized and prepared for immunohistochemical staining. The microinjected-site was assessed by checking histological sections. Only rats showing dyes spot in the NRM were considered for analysis.

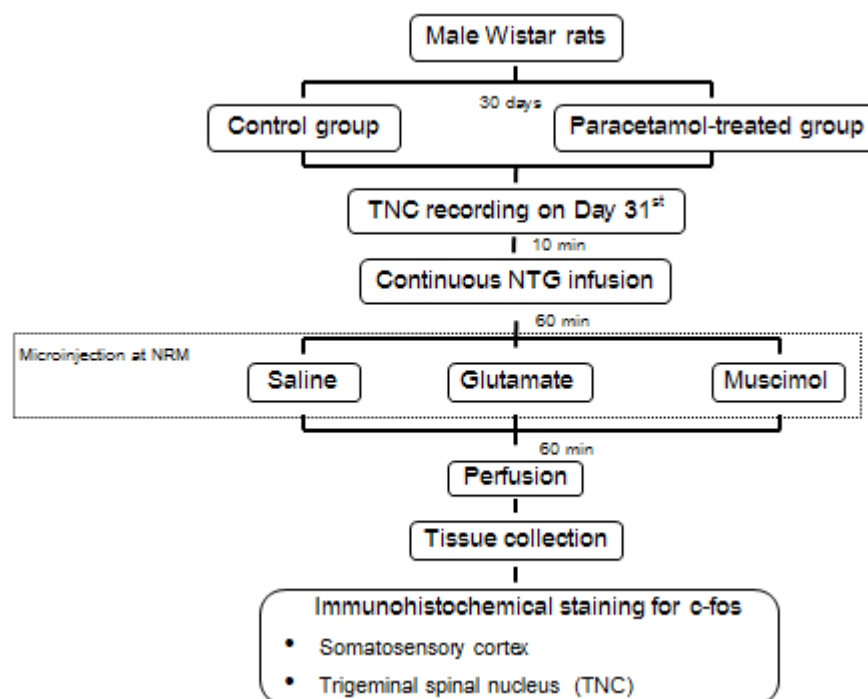


Figure 6 Experimental design 2

To examine an involvement of NRM on neuronal excitability in trigeminal nucleus caudalis of chronic paracetamol-treated rats after activated by nitroglycerin.

ANIMAL PREPARATION

Adult male Wistar rats weighing 180-200 g were purchased from the National Laboratory Animal Center of Salaya Campus, Mahidol University. These animals were housed in stainless-steel bottom cages 4-5 animals per cage at animal research center,

Faculty of Dentistry, Chulalongkorn University. The room temperature was 25-30 °C with 12:12 dark-light cycle. All animals were allowed to access food and tap water ad libitum. To limit the effect of nonspecific stress, all animals were accustomed to daily handling for at least 3 days before experimentation.

Rats were divided into 2 main groups, chronic paracetamol-treated and control groups. In paracetamol-treated rats, paracetamol (T.P. drug laboratories, Thailand) were injected intraperitoneally at a dose equivalent to 200 mg/kg while the control rats were given the 0.9% NaCl (Hospital Products Public, Thailand) as a vehicle. The volume of all drug injections was calculated according to standard criteria (intraperitoneally 10 ml/kg). All animals were received daily injection between 9.00-12.00 a.m. for 30 days. Based on the previous data from Yisarakun W. et al, there were no biochemical parameters of liver damage in paracetamol-treated rats at a dosage of 200 mg/kg for 30 days (80). They reported that the liver enzyme function in paracetamol-treated groups, including alanine aminotransferase (ALT), aspartate aminotransferase (AST) and alkaline phosphatase (ALP), did not show a significant difference compared with control group.

In each experimental protocol, the rats were anesthetized by intraperitoneal administration of sodium pentobarbital (Nembutal®, Sanofi, Thailand) at dose 60 mg/kg. Additional doses of anesthetics were given as required to maintain surgical anesthesia based on testing of corneal reflex and response to tail pinch. A tracheostomy was done to help the ventilation.

All procedures were approved by the Ethical Committee of Faculty of Dentistry, Chulalongkorn University (animal use protocol No. 1632001).

CHEMICAL PREPARATION

Glutamic acid (Sigma, USA) was dissolved in 0.9%NaCl to prepare 50 mM glutamate for microinjection. Muscimol solution (10 nM) for microinjection was prepared from Muscimol (Calbiochem, UK) which dissolved in 0.9%NaCl. All solutions for NRM microinjection were contained Pontamine Sky blue (Sigma, USA) (2.5% by weight). NTG

(Pharmaland, Thailand) was dissolved in 0.9%NaCl to prepare an intravenous NTG solution (0.5 mg/kg) on the day of experiment. Buffer solution stock (0.2 M) was prepared from 5.16g Potassium phosphate (KH_2PO_4) (Riedel-de Haën, Germany) and 22.98g Sodium phosphate (Na_2HPO_4) (Merck, Germany) in 1000 ml distilled water. On the day of experiment, equal parts of 0.2 M buffer solution stock and distilled water were mixed to prepare 0.1 M buffer solution. The 4% paraformaldehyde fixative was freshly prepared from adding equal parts of 8% paraformaldehyde fixative stock to 0.2 M buffer solution stock on the day of experiment. To prepare 8% paraformaldehyde fixative stock, paraformaldehyde (Sigma, USA) 40 g was dissolved in 500 ml distilled water. The solution was heat to 60-65°C while stirring. NaOH (Eka Nobel, Sweden) was added to clear the solution.

ELECTROPHYSIOLOGICAL RECORDING

1) CORTICAL SPREADING DEPRESSION MODEL

a. SURGICAL PREPARATION

After tracheostomy, the rat was placed on a surgical pad and its head was fixed on a stereotaxic frame (Singa technology corporation, Taiwan). Next, frontal and parietal bones were exposed by mobilization of skin from the midline incision. At the left side, the anterior craniotomy (diameter 5 mm) was performed using saline-cooled drill (NSK, Japan) at the coronal suture, 1 mm laterally from bregma. The posterior craniotomy (diameter 3 mm) was performed in the parietal bone at 7 mm posteriorly and 1 mm laterally from bregma. The anterior craniotomy was used for placing the electrode, while CSD was initiated from the posterior craniotomy opening (Figure 7). The dura was opened by needle (guage 27) under microscopic observation (Takagi, Japan). Normal saline was applied to clean and keep moist in the intracranial space. Solid KCl (3 mg) (Merck, Germany) was applied to the posterior craniotomy opening to initiate CSD.

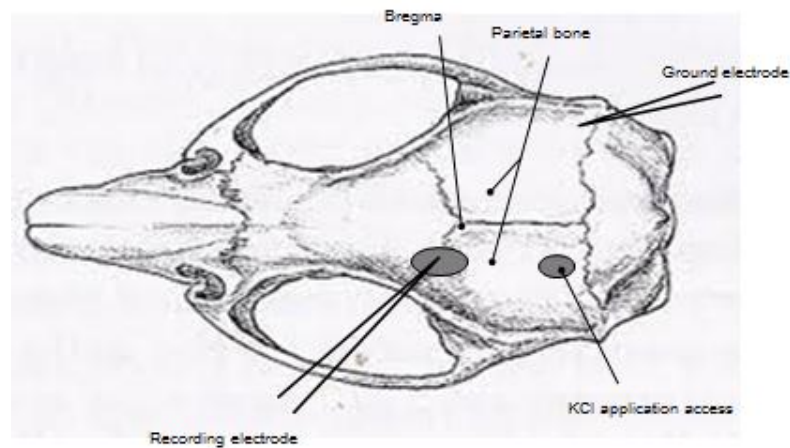


Figure 7 The surgical areas for electrocorticographic recording

The anterior craniotomy (diameter 5 mm) was performed at the coronal suture, 1 mm laterally from bregma for placing recording electrode. The posterior craniotomy (diameter 3 mm) was performed in the parietal bone at 7 mm posteriorly and 1 mm laterally from bregma for CSD initiation. Figure was adapted from Paxinos G. et al. (81).

To prepare microinjected-site, a midline rectangular craniotomy was made over the cerebellum by carefully grinding action (Figure 8). Next, microinjection needle was inserted into NRM by microsyringe manipulator. The coordinates for the NRM are -11.6 mm anterior/posterior, 0 mm lateral and -10.5 mm ventral from bregma (32). The 0.2 μ l solution of glutamate, muscimol or saline contained Pontamine sky blue was injected through a 5 μ l syringe (Hamilton, USA). Microinjections were controlled at a constant rate over 1 minute by microsyringe pump controller (World precision instrument, USA).

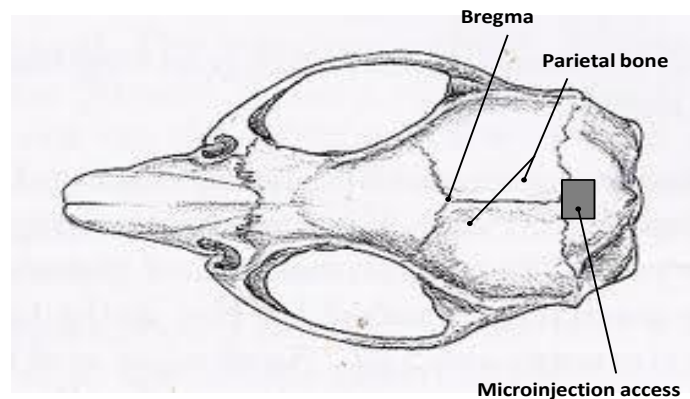


Figure 8 The surgical area for microinjection at nucleus raphe magnus

A midline rectangular craniotomy (diameter 5 mm) was made over the occipital bone at 10 mm posteriorly from bregma for placing microinjection needle. Figure was adapted from Paxinos G. et al. (81).

b. ELECTROCORTICOGRAPHIC RECORDING AND DATA COLLECTION

CSD wave was recorded as direct current (DC) shift by a recording electrode. The glass recording electrode was prepared from a micropipette puller (Sutter Instrument, CA, USA), filled with 4 M NaCl and fixed with digital storage oscilloscope and inserted perpendicularly to cortex to depth 1 mm from cortical surface by using a hydraulic micromanipulator (Narishige, Japan). A ground electrode was fixed as a reference point. The obtained electrical signal was amplified using microelectrode amplifier (IX2-700, Dagan, USA). Analog data were converted to a digital form using data acquisition system. All tracing were analyzed by using computer software (Labchart 8) (ADInstrument, Australia). Such waveform was continuously monitored for 30 minutes as baseline. Then, rats in control and paracetamol-treated groups were subdivided into two subgroups. Each subgroup was microinjected with 0.2 μ l glutamate, muscimol or saline at NRM and continuously recorded for 90 minutes.

2) NTG-INDUCED HEADACHE MODEL

a. SURGICAL PREPARATION

After tracheostomy, rats were cannulated at femoral artery and vein. The femoral artery was inserted a catheter contained saline to record blood pressure during the whole experiment, whereas the femoral vein catheter was prepared for NTG administration. The skin at C1-C2 areas was transected in the mid-sagittal plane. Then, the lamina process of C1 was removed. The medullary brainstem was exposed by cutting the underlying dura mater. Normal saline was used to clean and keep moist in the brainstem area.

A midline rectangular craniotomy was performed over the cerebellum to allow access to the NRM (Figure 8). The coordinates for the NRM are -11.6 mm anterior/posterior, 0 mm lateral and -10.5 mm ventral from bregma (32). The 0.2 μ l solution of glutamate, muscimol or saline contained Pontamine sky blue was injected through a Hamilton syringe which were controlled by a microsyringe pump controller.

b. EXTRACELLULAR RECORDING AT TNC AND DATA COLLECTION

Glass recording electrode filled with 4 M NaCl was advanced by microstepper into the left side of the TNC with reference to an atlas of the rat brain (16). Then, neurons were test for convergent input from peri-orbital skin at the left side by cotton rubbing. Also, neurons were identified their responding with a stable latency to electrical stimulation (0.5 Hz, 0.1 ms, 15-20 V) at middle meningeal artery. In this experiment, the response latency of neurons varied from 5-45 ms and a conduction distance is approximately 25 mm. These data suggested that the afferent input came from A-delta fiber (>2 m/s) or C-fiber (0.5-2 m/s). (Figure 9)

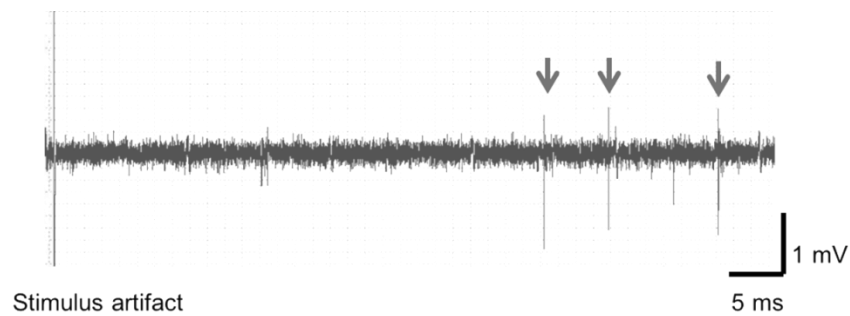


Figure 9 Example of spike latency of recording neurons

The arrows show the latencies of the spikes after electrical stimulation at middle meningeal artery. The conduction velocities indicate the afferent input from A-delta fiber or C-fiber.

The signals were amplified, bandpass (DP-311, Warner instruments, USA) and saved for offline analysis with labChart 8 software. Hum bug noise eliminator was used (Quest Scientific, UK). After identifying neuron in TNC, spontaneous activity of neurons in TNC was recorded for 10 minutes as a baseline. Then, NTG (0.5 mg/kg 1 ml) was infused at a constant rate of 0.5 ml/h to the femoral vein for 2 hours by using syringe pump controller (Harvard apparatus, USA). Neuronal activity was continuously monitored for two hours after NTG infusion. One hour after NTG infusion, rats in control and paracetamol-treated groups were subdivided into three subgroups. Each subgroup was microinjected with 0.2 μ l glutamate, muscimol or saline at NRM and continuously recorded the neuronal activity for 60 minutes. Data were shown in percent change from baseline value of the neuronal activity. Each rat was examined only one time. The position of each recording site was determined by measuring the distance from the obex and the depth from surface of brainstem.

IMMUNOHISTOCHEMICAL STUDY

1) PERFUSION AND TISSUE PREPARATION

After completion of CSD monitoring or single unit recording at TNC, animals were further proceeding for immunohistochemical study. The experimental rats were deeply anesthetized with sodium pentobarbital. Laparotomy and thoracotomy were done. A cannula was inserted into the apex of the heart and advanced distally to the

aortic arch. Then, the vasculature was flushed transcardially with 200 ml buffer solution, followed by 200 ml of 4% paraformaldehyde. Brain and the cervical spinal cord were removed and immediately immersed in 4% paraformaldehyde for 24 hours. Then, tissues were stored in buffer solution.

2) IMMUNOHISTOCHEMICAL STAINING FOR THE FOS

Brain sections (1-4 mm caudal from bregma) were processed and embedded in paraffin. Then, the 5 μm -thick paraffin sections were cut and mounted on positive-charge glass slides (Matsunami, Japan). The procedure for immunohistochemical staining in paraffin-embedded sections was shown in Figure 10. Firstly, the paraffin sections were deparaffinized and rehydrated. The slides were baked on the slide warmer at 60 °C for 15 minutes. Then, the slides were incubated with three changes of xylene, 5 minutes in each change. Next, the slides were incubated with two changes of 100% ethanol, one change of 95% ethanol and two changes of distilled water, 3 minutes in each change. To unmask the antigens, the slides were incubated in target retrieval solution, citrate buffer pH 6.0 (Dako, USA) and heated in microwave (Opticook, Moulinex, France) for 10 minutes. After that, the slides were cooled for 30 minutes at room temperature and rinsed two times with distilled water. Then, the slides were incubated in 3% H_2O_2 for 10 minutes, washed two times with distilled water and one time with PBS. To block the non-specific antigen, the slides were incubated in 3% normal horse serum in PBS for 60 minutes. After washed with PBS for three times, the sections were incubated with c-FOS specific antibody solution (1:50, code E 8, Santa Cruz, USA) at 4 °C overnight. Next, the slides were washed with PBS for 3 times and incubated with labeled polymer-HRP anti-mouse/rabbit (Envision system, Dako, USA) for 30 minutes, followed by PBS rinsing. After that, the slides were incubated in substrate containing 3,3'-Diaminobenzidine (DAB) (1 drop of DAB:1 ml of substrate) for 5 minutes. The reaction was stopped by washing with PBS. Finally, the slides were immersed in 95% ethanol, 100% ethanol and xylene before mounting with coverslips.

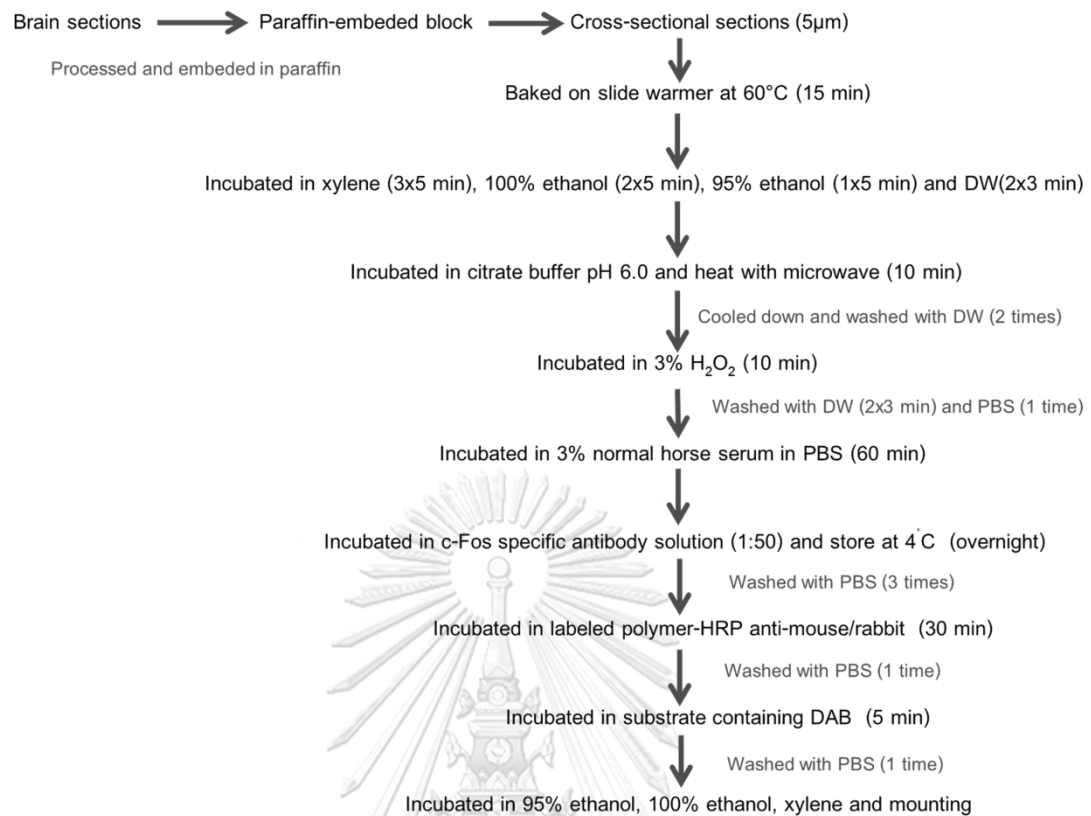


Figure 10 Fos staining protocol for paraffin-embedded sections of brain

The free-floating TNC sections were prepared for Fos immunohistochemical staining. The brief process was demonstrated in Figure 11. TNC (1.5 mm rostrally and 6 mm caudally from the tip of obex) was immersed in a 30% sucrose in buffer solution for 2 days before slices preparation. Next, TNC was cross-sectional cut by a cryostat microtome (Leika, Germany) at 30 µm thickness. Every third section from TNC was collected for Fos immunocytochemistry.

TNC sections were rinsed in three changes of PBS (Sigma, USA) to remove embedding media. Next, the sections were incubated with 50% ethanol (Merck, Germany) for 30 minutes and 3% hydrogen peroxide (Merck, Germany) in 50% ethanol for 30 minutes to block endogenous peroxidase. After repeated rinses in PBS, the non-specific binding of the antibody was blocked by incubating the tissues with a 3% normal horse serum (Invitrogen, New Zealand) in PBS for 60 minutes at room temperature. After washed with PBS for three times, the sections were incubated in the c-Fos specific

antibody solution (1:1000, code SC52, Santa Cruz, USA) at 4 °C. After overnight incubation, the sections were rinsed three times with PBS. Then, the sections were incubated with labeled polymer-HRP anti-rabbit (Envision system, Dako, USA) for 30 minutes, followed by PBS rinsing. Afterwards, all sections were incubated in substrate containing DAB (1 drop of DAB:1 ml of substrate) for 10 minutes. The reaction was stopped by washing with PBS. Finally, these sections were mounted on glass slides, air-dried and covered with coverslips.

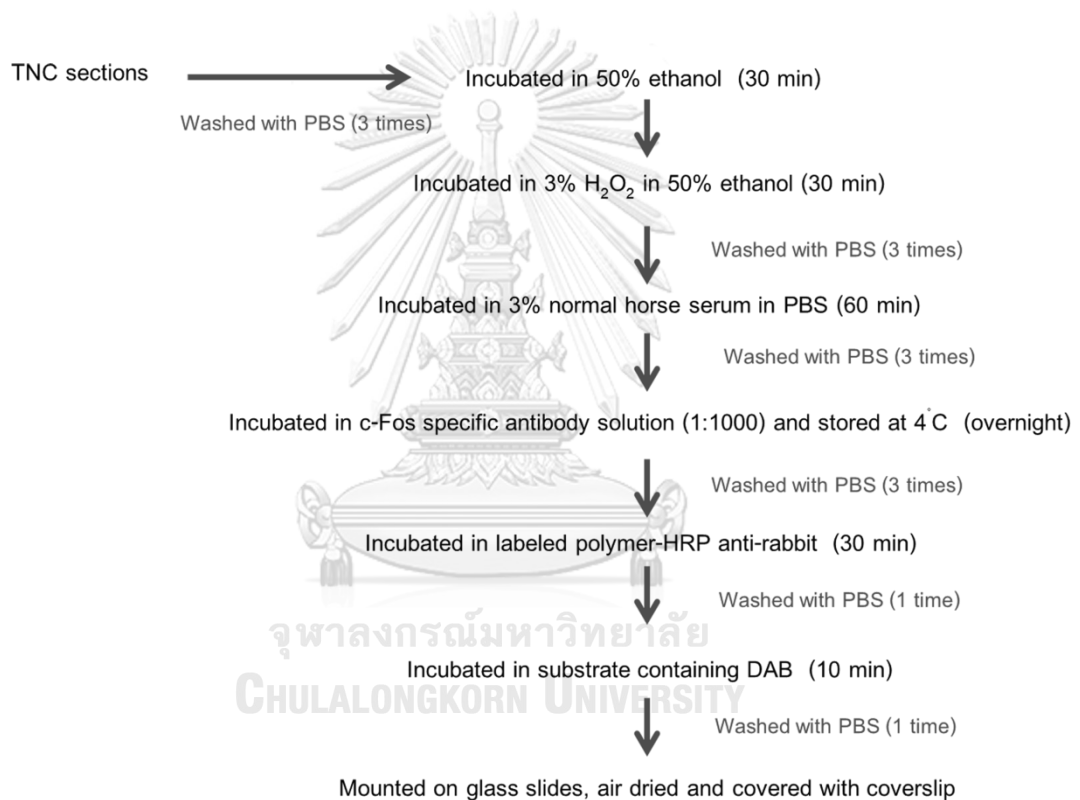


Figure 11 Fos staining protocol for free-floating sections of trigeminal nucleus caudalis

3) DATA COLLECTION FOR THE IMMUNOREACTIVE CELLS

Two brain sections (the first and the seventh of brain sections) were scanned using Aperio ScanScope slide scanner (Leica, USA). Each brain section was drawn an outline on primary somatosensory cortex (barrel field region) area (Figure 12). Then, the c-Fos immunoreactive cells (Fos-IR cells) in the outline was counted using

Aperio ScanScope software (Leica, USA). This program separated Fos-IR cells into three levels, 1+, 2+ and 3+, depending on their color intensity. Only Fos-IR cells which showed the highest intensity (3+) were counted in this study.

Alternatively, the numbers of immunoreactive cells in the lamina I and the lamina II areas of TNC for 20 slices were counted manually by using a light microscope (Figure 12). Only cell profiles with a visible staining on the focal plane were analyzed. The Fos-IR cells were defined as those with a dark brown stain in their nucleus. Furthermore, the Fos-IR cells in ipsilateral and contralateral side of CSD induction were counted separately.

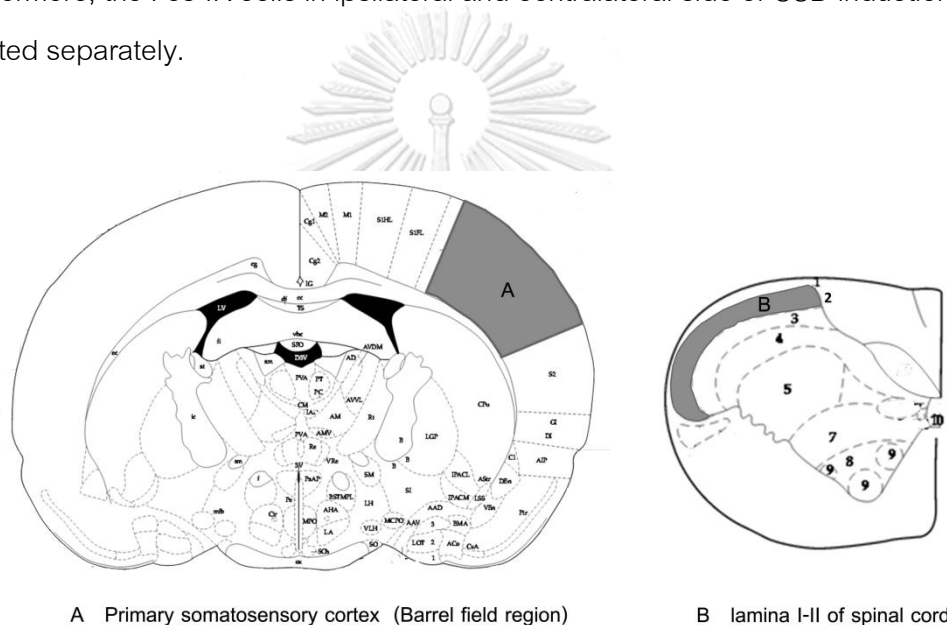


Figure 12 Areas for data collection at cortex and trigeminal nucleus caudalis

Figures came from Paxinos G. et al. (81).

DATA ANALYSIS

All data were presented as mean±standard deviation (SD). Statistical analysis was performed using Kruskal-Wallis H test, Mann-Whitney U test and Willcoxon Rank Sum test. Statistical significant was set at $p < 0.05$. The computer software SPSS version 22 for windows was used to analyse all data.

CHAPTER 4

RESULTS

This study comprises two experiments in order to investigate an involvement of NRM on the neuronal excitability at cortex and TNC in long term paracetamol-treated rats.

EXPERIMENT 1: To examine an involvement of NRM on CSD-evoked neuronal excitability of chronic paracetamol-treated rats

The average body weights of rats were 365.4 ± 37.0 g and 346.0 ± 15.2 g in control (N=22) and paracetamol-treated (N=21) groups, respectively. There were no statistically changed in rats' body weights among these two groups ($P=0.127$). The animal behavior did not differ between control and paracetamol-treated groups.

MICROINJECTION AREA

The microinjected-site within NRM was assessed by checking histological sections with a microscope after finishing the experiment. Animals which were microinjected outside of the NRM were dismissed of this work. The sites of microinjection needles in both control and paracetamol-treated groups were demonstrated in Figure 13.

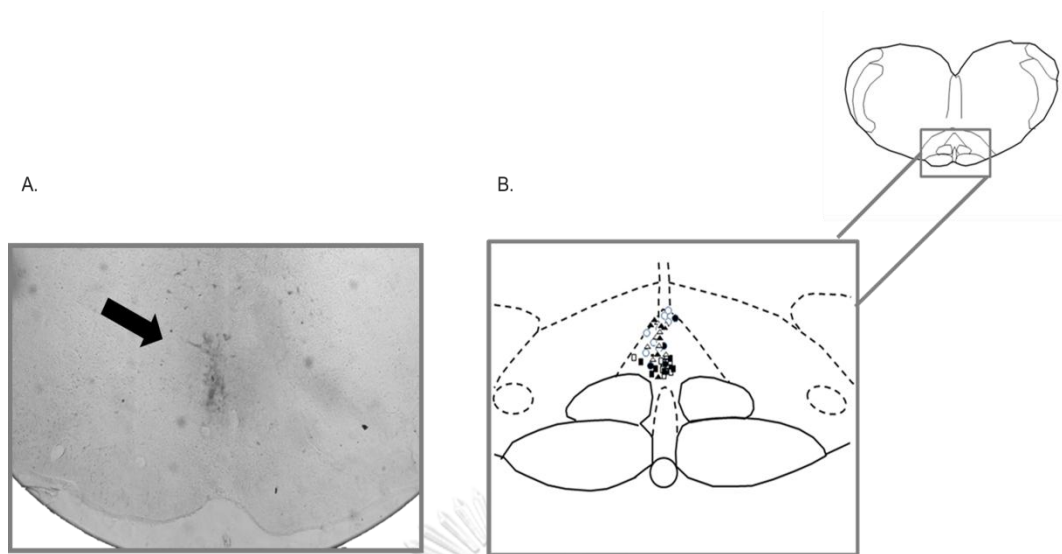


Figure 13 Schematic of microinjected-site at nucleus raphe magnus in experiment 1

A. Photomicrograph represents the microinjected-site at nucleus raphe magnus. B. Schematic of microinjection sites in both control and paracetamol-treated groups. White circle, control group with saline microinjection; White triangle, control group with glutamate microinjection; White square, control group with muscimol microinjection; Black circle, paracetamol-treated group with saline microinjection; Black triangle, paracetamol-treated group with glutamate microinjection; Black square, paracetamol-treated group with muscimol microinjection.

ELECTROCORTICOGRAPHIC RECORDING

The change of direct current (DC) shift was observed to evaluate the CSD development. A series of CSD wave was recorded within 2 hours after CSD initiation (Figure 14). NRM microinjection was generated 30 minutes after CSD initiation. The number of CSD wave was assessed.

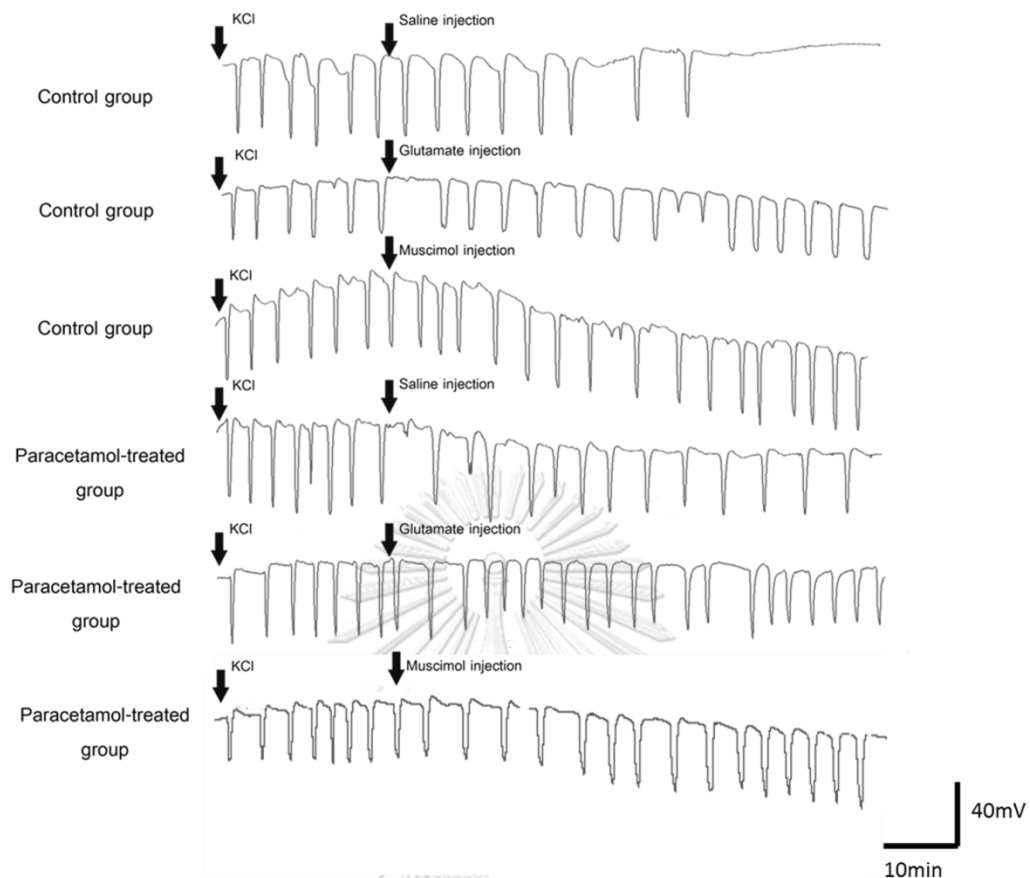


Figure 14 Effect of chronic paracetamol exposure on CSD development and modulating effect of microinjection into nucleus raphe magnus.

Chronic exposure to paracetamol significantly increased the number of CSD wave during the 30-minute baseline period. Muscimol injection increased the number of CSD wave in control group compared to saline injection. This effect was absent in rats with chronic paracetamol treatment.

Chronic exposure to paracetamol significantly increased the number of CSD wave during the 30-minute baseline period. The number of baseline CSD wave observed in the paracetamol-treated and control groups were 6.7 ± 1.0 and 5.7 ± 1.0 waves, respectively ($P=0.003$).

Ninety minutes post-saline microinjection, the number of CSD wave in paracetamol-treated group was still higher than in control group ($N=7$, 18.4 ± 5.8 waves and $N=7$, 10.9 ± 3.4 waves respectively; $P=0.015$). In control group, the number of CSD wave after the glutamate microinjection did not differ compared with the saline

microinjection group (N=8, 10.8 ± 2.2 waves; $P=0.958$). On the other hand, muscimol microinjection in control group increased the number of CSD wave (N=7, 15.7 ± 4.4 waves; $P=0.041$). However, the enhancing effect of muscimol on CSD development was not seen in the paracetamol-treated group (N=6, 17.3 ± 5.6 waves; $P=0.738$). Furthermore, the total numbers of CSD wave 90 minutes after glutamate microinjection in the paracetamol-treated group were 17.3 ± 2.4 waves (N=8, $P=0.632$). The numbers of CSD wave within 90 minutes post-microinjection were demonstrated in Figure 15. Data were shown in Table 1

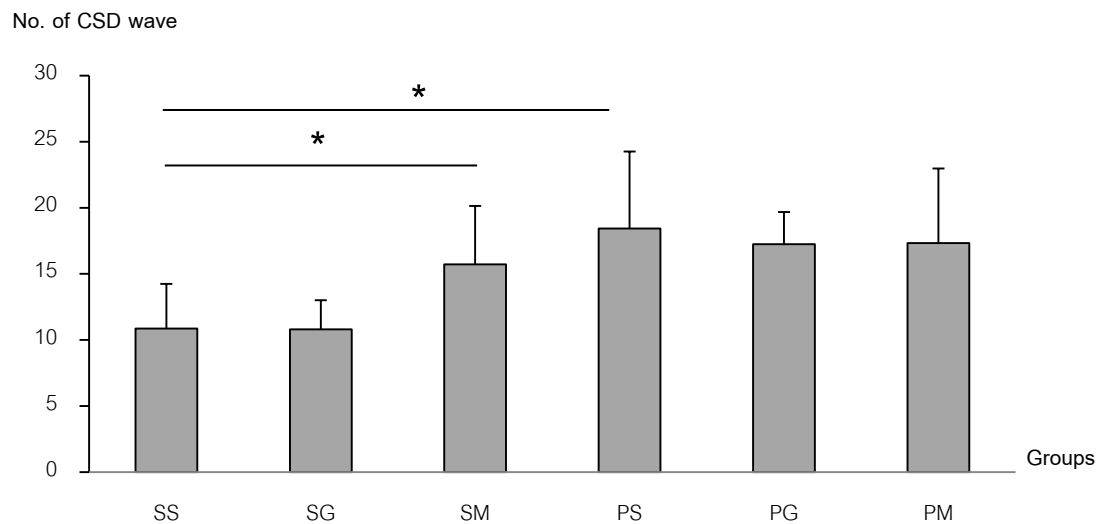


Figure 15 Effect of chronic paracetamol exposure on the number of CSD waves and modulating effect of microinjection into nucleus raphe magnus.

The number of CSD wave in paracetamol-treated group was still higher than in control group after saline microinjection. Muscimol injection increased the number of CSD wave in control group compared to saline injection. This effect was absent in rats with chronic paracetamol treatment.

* $P < 0.05$ compared between groups. SS: control with saline microinjection group. SG: control with glutamate microinjection group. SM: control with muscimol microinjection group. PS: paracetamol-treated with saline microinjection group. PG: paracetamol-treated with glutamate microinjection group. PM: paracetamol-treated with muscimol microinjection group.

Table 1 The average numbers of CSD wave after microinjection at nucleus raphe magnus area

	Control group			Paracetamol-treated group		
	Saline injection	Glutamate injection	Muscimol injection	Saline injection	Glutamate injection	Muscimol injection
Number of CSD wave	10.9±3.4	10.8±2.2	15.7±4.4*	18.4±5.8*	17.3±2.4	17.3±5.6

* $P < 0.05$ compared to control group with saline microinjection

CSD-EVOKED FOS EXPRESSION

In primary somatosensory cortex, the numbers of Fos-IR cells were shown in Table 2 and Figure 16-19. Fos-IR cells in ipsilateral and contralateral side to CSD induction were counted separately. The results showed that the number of Fos-IR cells in ipsilateral side to CSD induction was significantly greater than Fos-IR cells in contralateral side. Chronic paracetamol exposure was shown to increase the number of CSD-evoked Fos expression in the ipsilateral cortex compared with control rats (486.6 ± 63.2 and 346.8 ± 58.0 cells/mm² respectively, $P = 0.050$). Though, the number of Fos-IR cells in the contralateral cortex observed in these two groups was not significantly different (87.3 ± 60.0 and 28.2 ± 8.9 cells/mm² respectively, $P = 0.229$).

Focusing on the ipsilateral side of control group, the number of Fos-IR cells on the ipsilateral cortex significantly increased after muscimol microinjection compared with saline microinjection at NRM (554.4 ± 74.4 and 346.8 ± 58.0 cells/mm² respectively, $P = 0.050$). However, the difference was not found in glutamate-injected group compared with saline-injected group (335.7 ± 30.7 and 346.8 ± 58.0 cells/mm² respectively, $P = 0.788$).

In paracetamol-treated group, glutamate microinjection did not change the number of Fos-IR cells in ipsilateral cortex compared with saline microinjection (522.9 ± 180.6 and 486.6 ± 63.2 cells/mm² respectively, $P = 0.827$). Also, the number of

Fos-IR cells after muscimol microinjection was not significant different compared with saline microinjection (563.5 ± 13.6 and 486.6 ± 63.2 cells/ mm^2 respectively, $P=0.275$) (Figure 19)



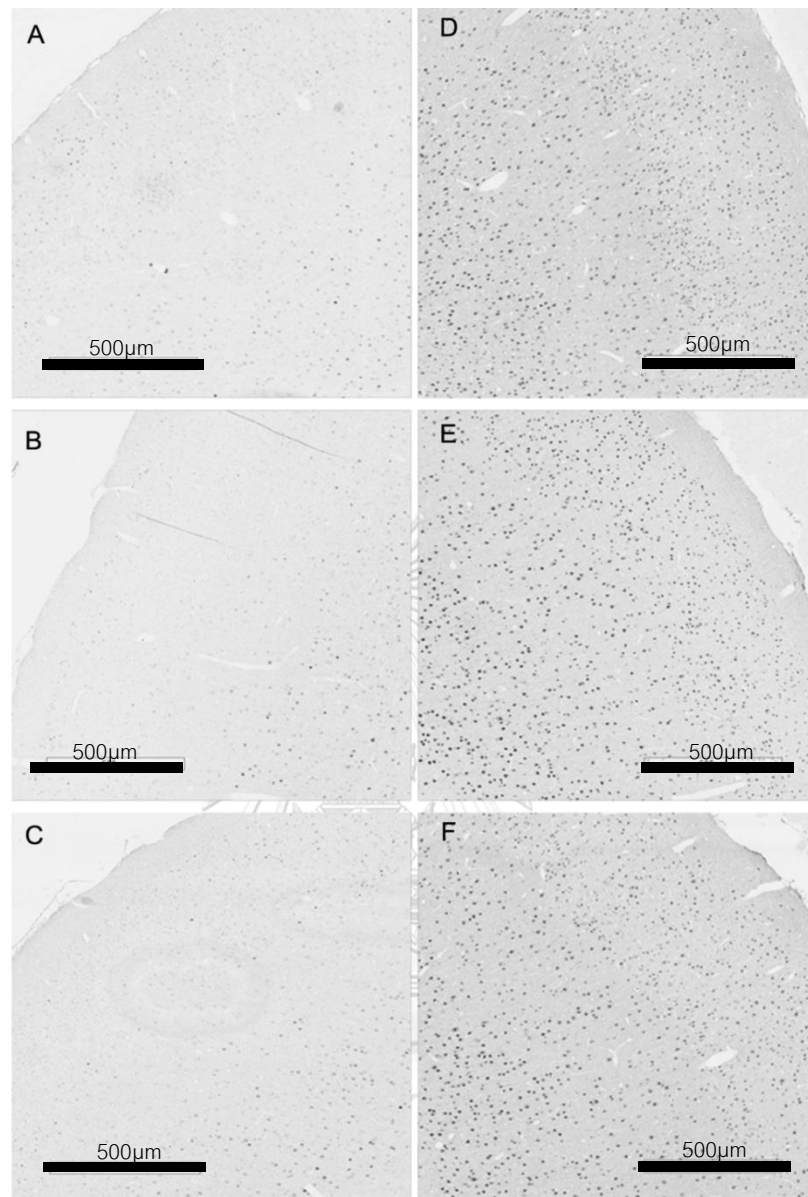


Figure 16 Photomicrograph shows the effect of CSD-evoked Fos expression in primary somatosensory cortex of control groups.

The number of Fos-IR cells in ipsilateral side to CSD induction was significantly greater than Fos-IR cells in contralateral side of control groups. A: contralateral cortex of control with saline microinjection group. B: contralateral cortex of control with glutamate microinjection group. C: contralateral cortex of control with muscimol microinjection group. D: ipsilateral cortex of control with saline microinjection group. E: ipsilateral cortex of control with glutamate microinjection group. F: ipsilateral cortex of control with muscimol microinjection group.

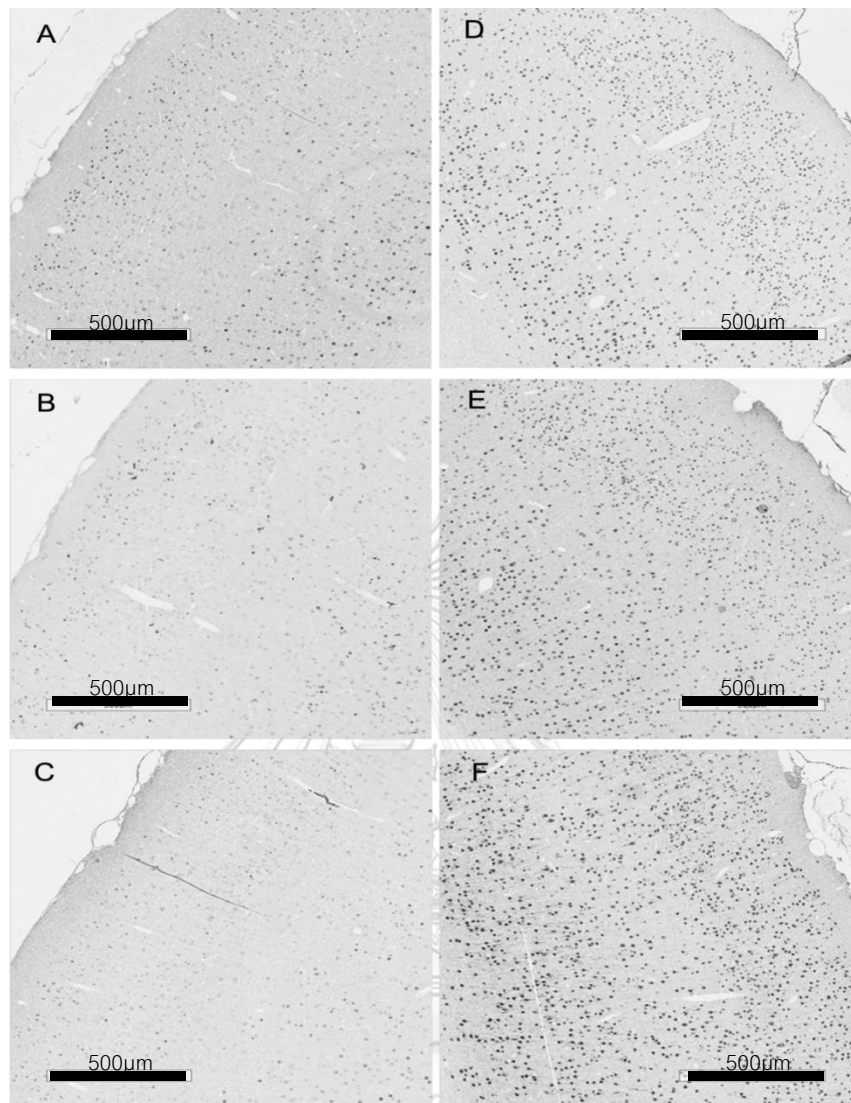


Figure 17 Photomicrograph shows the effect of CSD-evoked Fos expression in primary somatosensory cortex of paracetamol-treated groups

The number of Fos-IR cells in ipsilateral side to CSD induction was significantly greater than Fos-IR cells in contralateral side of paracetamol-treated groups. A: contralateral cortex of paracetamol-treated with saline microinjection group. B: contralateral cortex of paracetamol-treated with glutamate microinjection group. C: contralateral cortex of paracetamol-treated with muscimol microinjection group. D: ipsilateral cortex of paracetamol-treated with saline microinjection group. E: ipsilateral cortex of paracetamol-treated with glutamate microinjection group. F: ipsilateral cortex of paracetamol-treated with muscimol microinjection group.

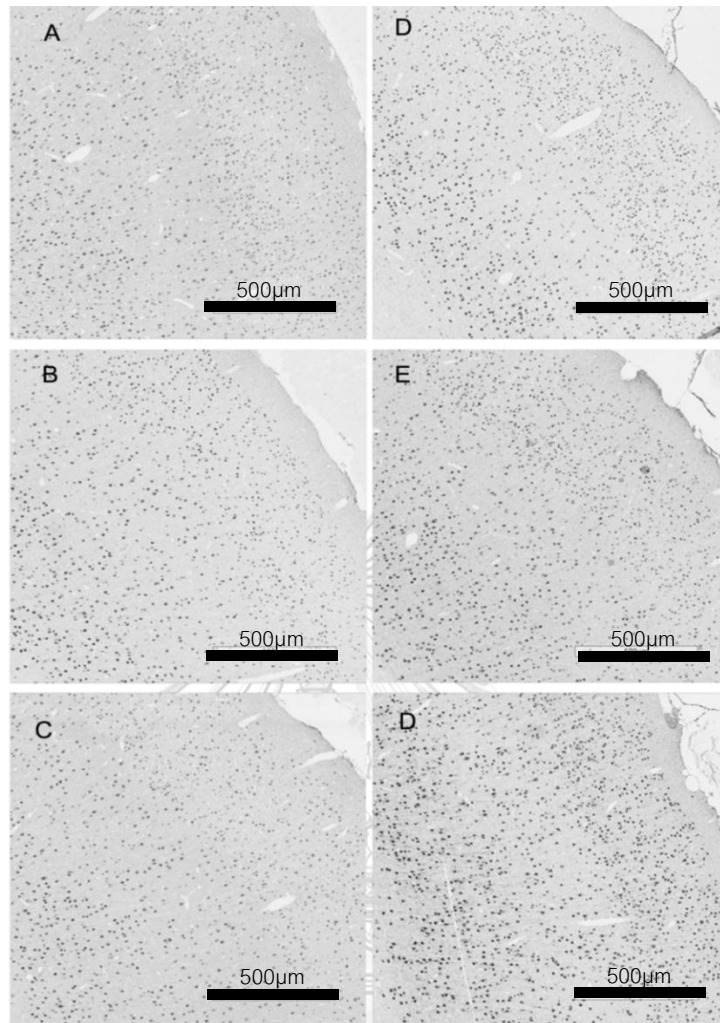


Figure 18 Photomicrograph shows the effect of chronic paracetamol exposure and modulating effect of microinjection into nucleus raphe magnus on CSD-evoked Fos expression in primary somatosensory cortex.

Chronic paracetamol exposure was shown to increase the number of CSD-evoked Fos expression in the ipsilateral cortex compared with control group. In control group, the number of Fos-IR cells on the ipsilateral cortex significantly increased after muscimol microinjection compared with saline microinjection at nucleus raphe magnus. In paracetamol-treated group, the difference was not found after muscimol microinjection compared with saline microinjection. A: control with saline microinjection group. B: control with glutamate microinjection group. C: control with muscimol microinjection group. D: paracetamol-treated with saline microinjection group. E: paracetamol-treated with glutamate microinjection group. F: paracetamol-treated with muscimol microinjection group

Table 2 The average numbers of CSD-evoked Fos expression in cortical neuron of primary somatosensory cortex

CSD-evoked Fos expression	Control groups			Paracetamol groups		
	Saline injection	Glutamate injection	Muscimol injection	Saline injection	Glutamate injection	Muscimol injection
Ipsilateral						
side (cells/mm ²)	346.8±58.0	335.7±30.7	554.4±74.4**	486.6±63.2**	522.9±180.6	563.5±13.6
Contralateral						
side (cells/mm ²)	28.2±8.9*	51.5±43.5*	74.6±10.7*	120.6±30.4*	103.6±66.7*	65.9±33.6*

* $P < 0.05$ compared between ipsilateral and contralateral side of CSD induction within group, ** $P < 0.05$ compared to control group with saline microinjection

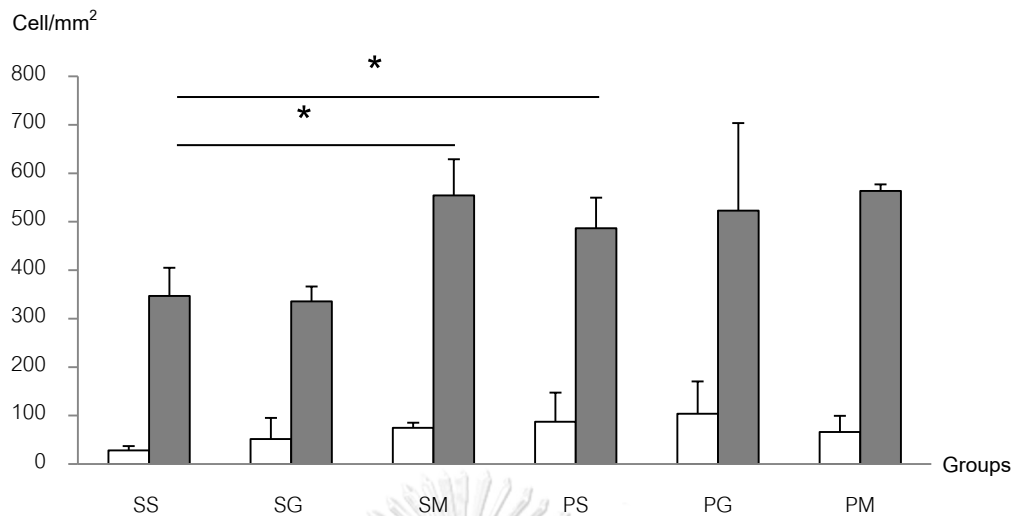


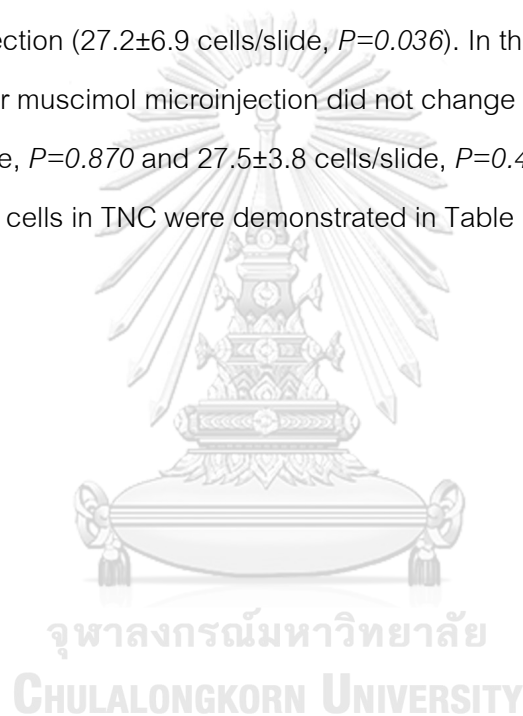
Figure 19 Effects of chronic paracetamol exposure and modulating effect of microninjection into nucleus raphe magnus on CSD-evoked Fos expression in primary somatosensory cortex.

Chronic paracetamol exposure was shown to increase the number of CSD-evoked Fos expression in the ipsilateral cortex compared with control group. In control group, the number of Fos-IR cells on the ipsilateral cortex significantly increased after muscimol microinjection compared with saline microinjection at nucleus raphe magnus. In paracetamol-treated group, the difference was not found after muscimol microinjection compared with saline microinjection. * $P < 0.05$ compared ipsilateral side of CSD induction between groups, the number of Fos-IR cells in ipsilateral side to CSD induction was significantly greater than contralateral side in all group ($P < 0.05$). Gray bar, Fos-IR cells in ipsilateral side of CSD induction; White bar, Fos-IR cells in contralateral side of CSD induction; SS: control with saline microinjection group. SG: control with glutamate microinjection group. SM: control with muscimol microinjection group. PS: paracetamol-treated with saline microinjection group. PG: paracetamol-treated with glutamate microinjection group. PM: paracetamol-treated with muscimol microinjection group.

At TNC, Fos-IR cells in ipsilateral and contralateral side to CSD induction were counted separately. The results showed that the number of Fos-IR cells in ipsilateral side to CSD induction was significantly greater than Fos-IR cells in contralateral side (Figure 20-22). In addition, it was found that paracetamol-treated rats were increased Fos expression in ipsilateral side of CSD induction (Figure 23, $P = 0.011$). The numbers of

Fos-IR cells at ipsilateral TNC were 30.0 ± 6.6 and 20.0 ± 3.4 cells/slide in the paracetamol-treated and control groups with NRM saline-microinjection respectively. On the other hand, Fos-IR cells in the contralateral TNC was not altered compared between paracetamol-treated and control groups (20.3 ± 7.8 and 13.5 ± 5.2 cells/slide respectively, $P=0.103$).

Focusing on the ipsilateral side, microinjection with glutamate did not change the number of Fos-IR cells as compared to the saline microinjection in the control group (20.9 ± 1.8 cells/slide, $P=0.546$). However, the number of Fos-IR cells was increased after muscimol microinjection (27.2 ± 6.9 cells/slide, $P=0.036$). In the paracetamol-treated group, glutamate or muscimol microinjection did not change the number of Fos-IR cells (29.4 ± 5.3 cells/slide, $P=0.870$ and 27.5 ± 3.8 cells/slide, $P=0.436$ respectively). The averages of Fos-IR cells in TNC were demonstrated in Table 3 and Figure 23.



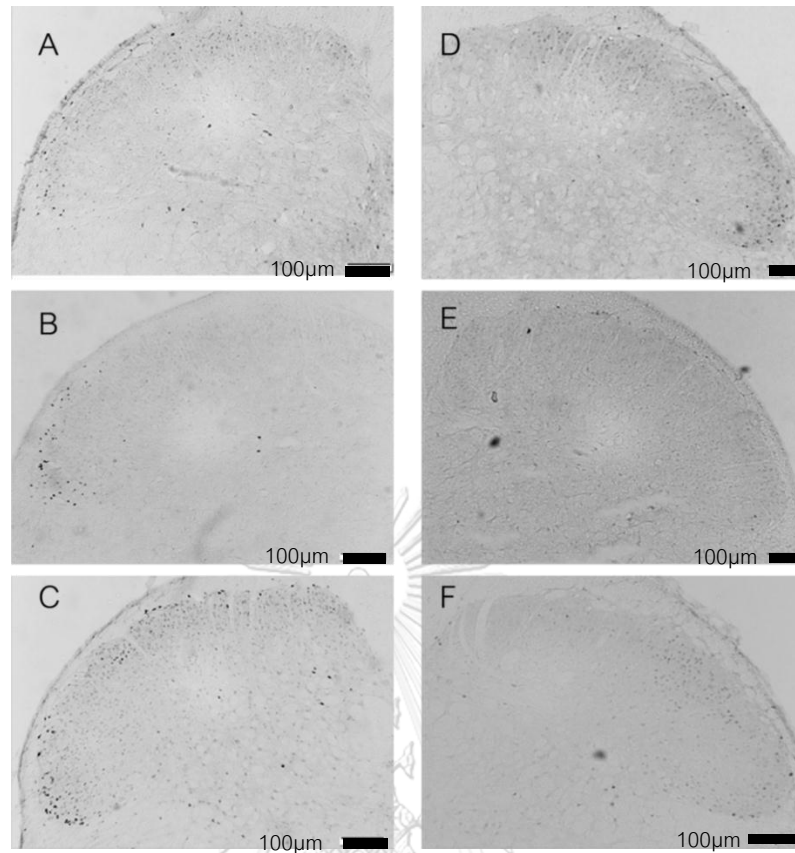


Figure 20 Photomicrograph shows the effect of CSD-evoked Fos expression in trigeminal nucleus caudalis of control groups.

The number of Fos-IR cells in ipsilateral side to CSD induction was significantly greater than Fos-IR cells in contralateral side of control groups. A: ipsilateral TNC of control with saline microinjection group. B: ipsilateral TNC of control with glutamate microinjection group. C: ipsilateral TNC of control with muscimol microinjection group. D: contralateral TNC of control with saline microinjection group. E: contralateral TNC of control with glutamate microinjection group. F: contralateral TNC of control with muscimol microinjection group.

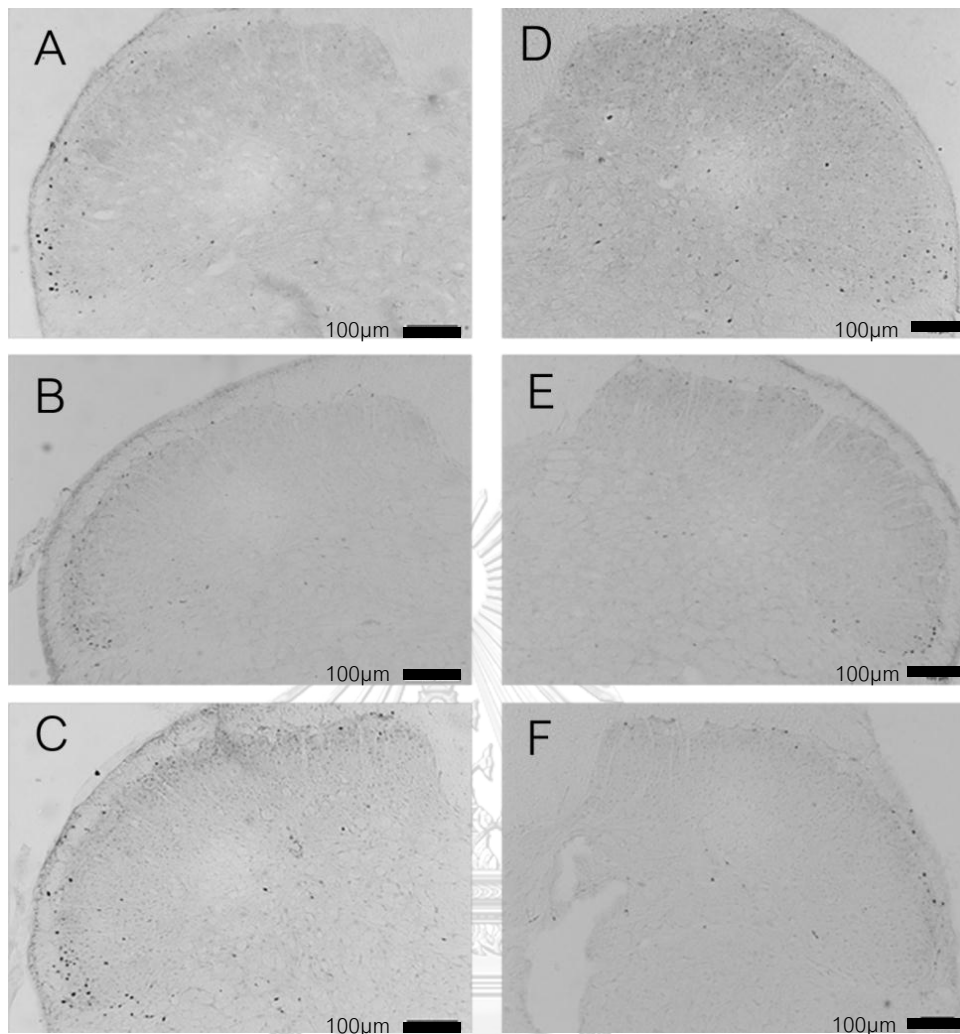


Figure 21 Photomicrograph shows the effect of CSD-evoked Fos expression in trigeminal nucleus caudalis of paracetamol-treated groups.

The number of Fos-IR cells in ipsilateral side to CSD induction was significantly greater than Fos-IR cells in contralateral side of paracetamol-treated groups. A: ipsilateral TNC of paracetamol-treated with saline microinjection group. B: ipsilateral TNC of paracetamol-treated with glutamate microinjection group. C: ipsilateral TNC of paracetamol-treated with muscimol microinjection group. D: contralateral TNC of paracetamol-treated with saline microinjection group. E: contralateral TNC of paracetamol-treated with glutamate microinjection group. F: contralateral TNC of paracetamol-treated with muscimol microinjection group.

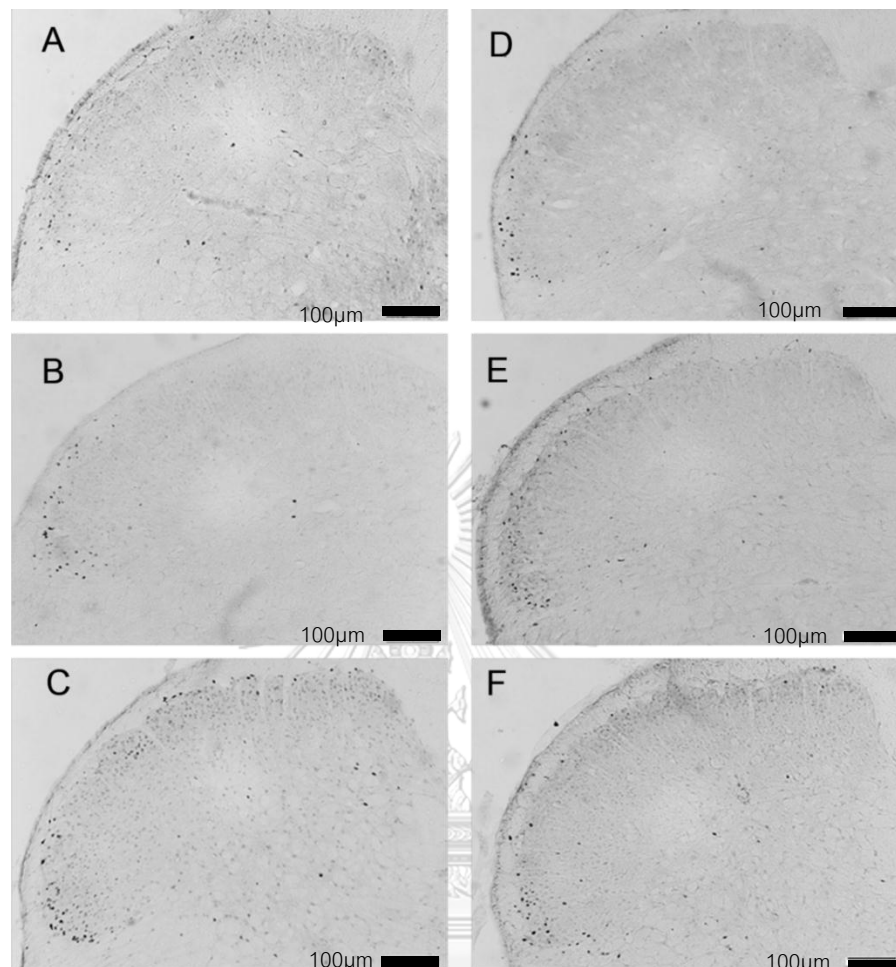


Figure 22 Photomicrograph shows the effects of chronic paracetamol exposure and modulating effect of microinjection into nucleus raphe magnus on CSD-evoked Fos expression in trigeminal nucleus caudalis.

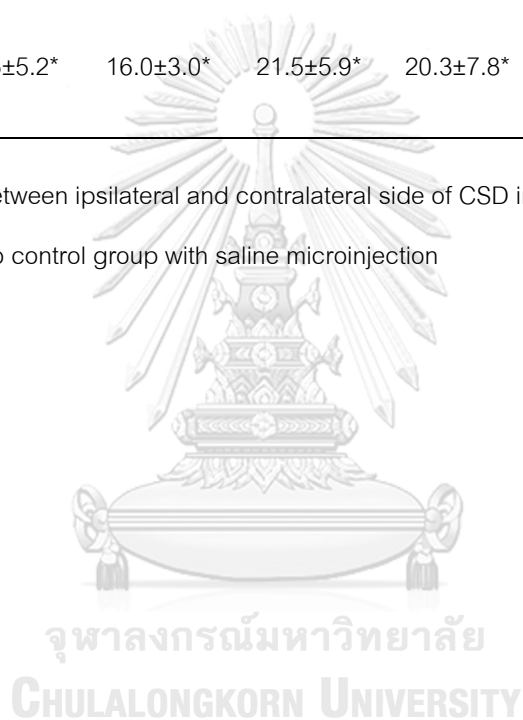
Chronic paracetamol exposure was shown to increase the number of CSD-evoked Fos expression in the ipsilateral TNC compared with control group. In control group, the number of Fos-IR cells on the ipsilateral TNC significantly increased after muscimol microinjection compared with saline microinjection at nucleus raphe magnus. In paracetamol-treated group, the difference was not found after muscimol microinjection compared with saline microinjection. A: control with saline microinjection group. B: control with glutamate microinjection group. C: control with muscimol microinjection group. D: paracetamol-treated with saline microinjection group. E: paracetamol-treated with glutamate microinjection group. F: paracetamol-treated with muscimol microinjection group

Table 3 The average numbers of CSD-evoked Fos expression in neurons of trigeminal nucleus caudalis

CSD-evoked Fos expression	Control group			Paracetamol-treated group		
	Saline injection	Glutamate injection	Muscimol injection	Saline injection	Glutamate injection	Muscimol injection
Ipsilateral side (cells/slide)	20.0±3.4	20.9±1.8	27.2±6.9**	30.0±6.6**	29.4±5.3	27.5±3.8
Contralateral side (cells/slide)	13.5±5.2*	16.0±3.0*	21.5±5.9*	20.3±7.8*	22.6±4.7*	17.7±3.3*

* $P < 0.05$ compared between ipsilateral and contralateral side of CSD induction within group,

** $P < 0.05$ compared to control group with saline microinjection



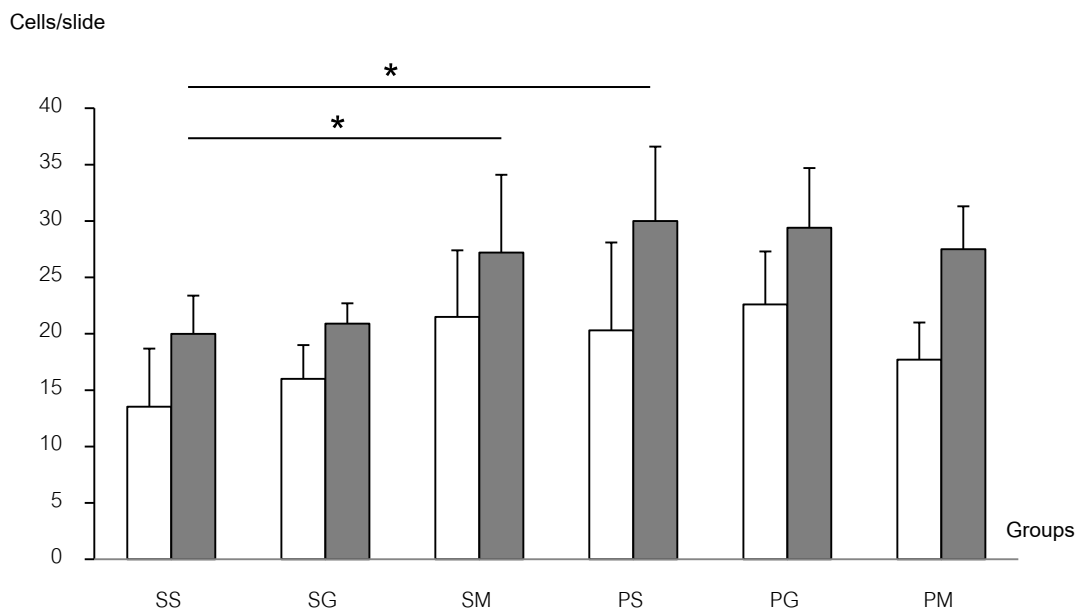


Figure 23 Effects of chronic paracetamol exposure and modulating effect of microninjection into nucleus raphe magnus on CSD-evoked Fos expression in trigeminal nucleus caudalis.

Chronic paracetamol exposure was shown to increase the number of CSD-evoked Fos expression in the ipsilateral TNC compared with control group. In control group, the number of Fos-IR cells on the ipsilateral TNC significantly increased after muscimol microinjection compared with saline microinjection at nucleus raphe magnus. In paracetamol-treated group, the difference was not found after muscimol microinjection compared with saline microinjection. $*P < 0.05$ compared ipsilateral side of CSD induction between groups, the number of Fos-IR cells in ipsilateral side to CSD induction was significantly greater than contralateral side in all group ($P < 0.05$). Gray bar, Fos-IR cells in ipsilateral side of CSD induction; White bar, Fos-IR cells in contralateral side of CSD induction; SS: control with saline microinjection group. SG: control with glutamate microinjection group. SM: control with muscimol microinjection group. PS: paracetamol-treated with saline microinjection group. PG: paracetamol-treated with glutamate microinjection group. PM: paracetamol-treated with muscimol microinjection group

EXPERIMENT 2: To examine an involvement of NRM on NTG-induced neuronal excitability of chronic paracetamol-treated rats

The average body weights of rats were 342.6 ± 22.9 g and 353.3 ± 23.9 g in control (N=24.) and paracetamol-treated (N=23) groups respectively. There were no statistically changed in rats' body weights among these two groups ($P=0.578$).

MICROINJECTION AREA

The microinjected-site within NRM was assessed by checking histological sections with a microscope after finishing the experiment. Animals which were microinjected outside of the NRM were dismissed of this work. The sites of microinjection needles in all groups were shown Figure 24.

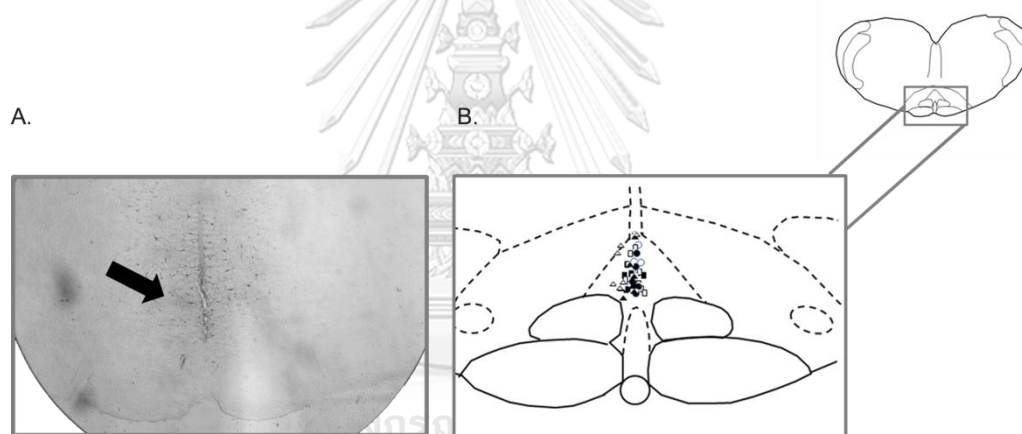


Figure 24 Schematic of microinjected-site at nucleus raphe magnus in experiment 2

A. Photomicrograph represents the microinjected-site at nucleus raphe magnus. B. Schematic of microinjection sites in both control and paracetamol-treated groups. White circle, control group with saline microinjection; White triangle, control group with glutamate microinjection; White square, control group with muscimol microinjection; Black circle, paracetamol-treated group with saline microinjection; Black triangle, paracetamol-treated group with glutamate microinjection; Black square, paracetamol-treated group with muscimol microinjection

EXTRACELLULAR RECORDING

Recording sites were located in an area 2.0-4.5 mm caudal to the obex, 0.8-2.5 mm lateral to the midline and 0.2-1.0 mm from the surface of the brainstem.

The spontaneous neuronal activity was monitored 10 minutes as baseline before 120 minutes NTG infusion. NRM microinjection was started 60 minutes after NTG infusion. The example of TNC firing rate in control and paracetamol-treated rats within 130 minutes were demonstrated in Figure 25-26.

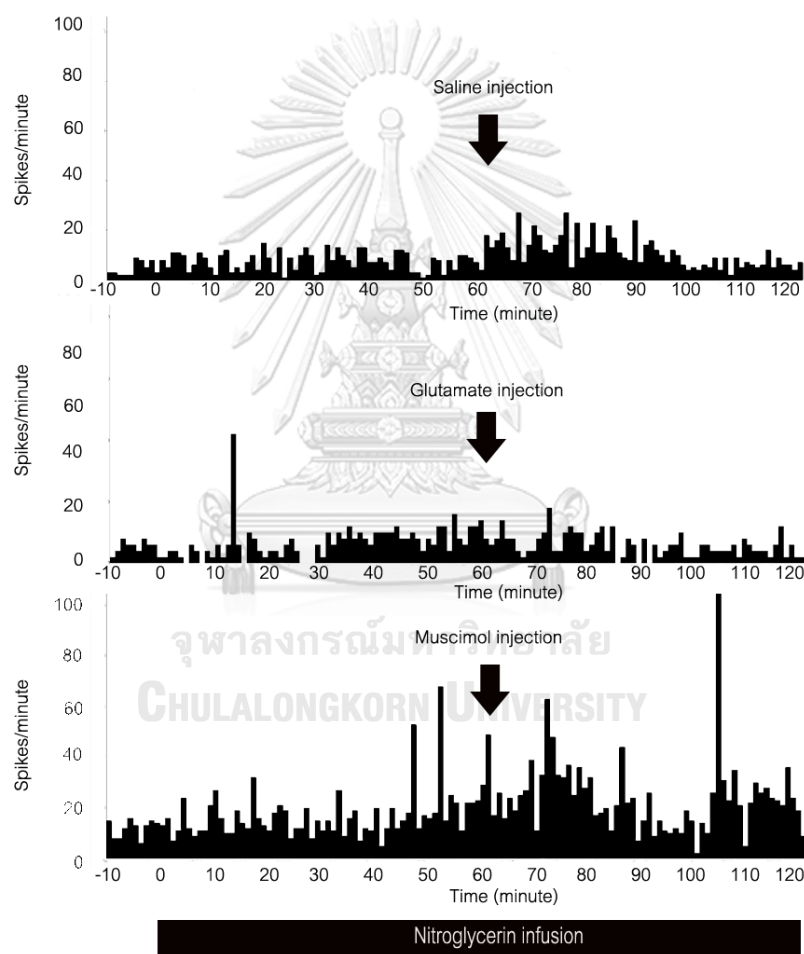


Figure 25 Modulating effect of microinjection into nucleus raphe magnus on nitroglycerin-evoked neuronal firing in trigeminal nucleus caudalis (representative records of patterns of TNC firing).

In control rats, glutamate microinjection decreased the TNC firing whereas muscimol microinjection was shown to increase the number of TNC firing compared with saline microinjection.

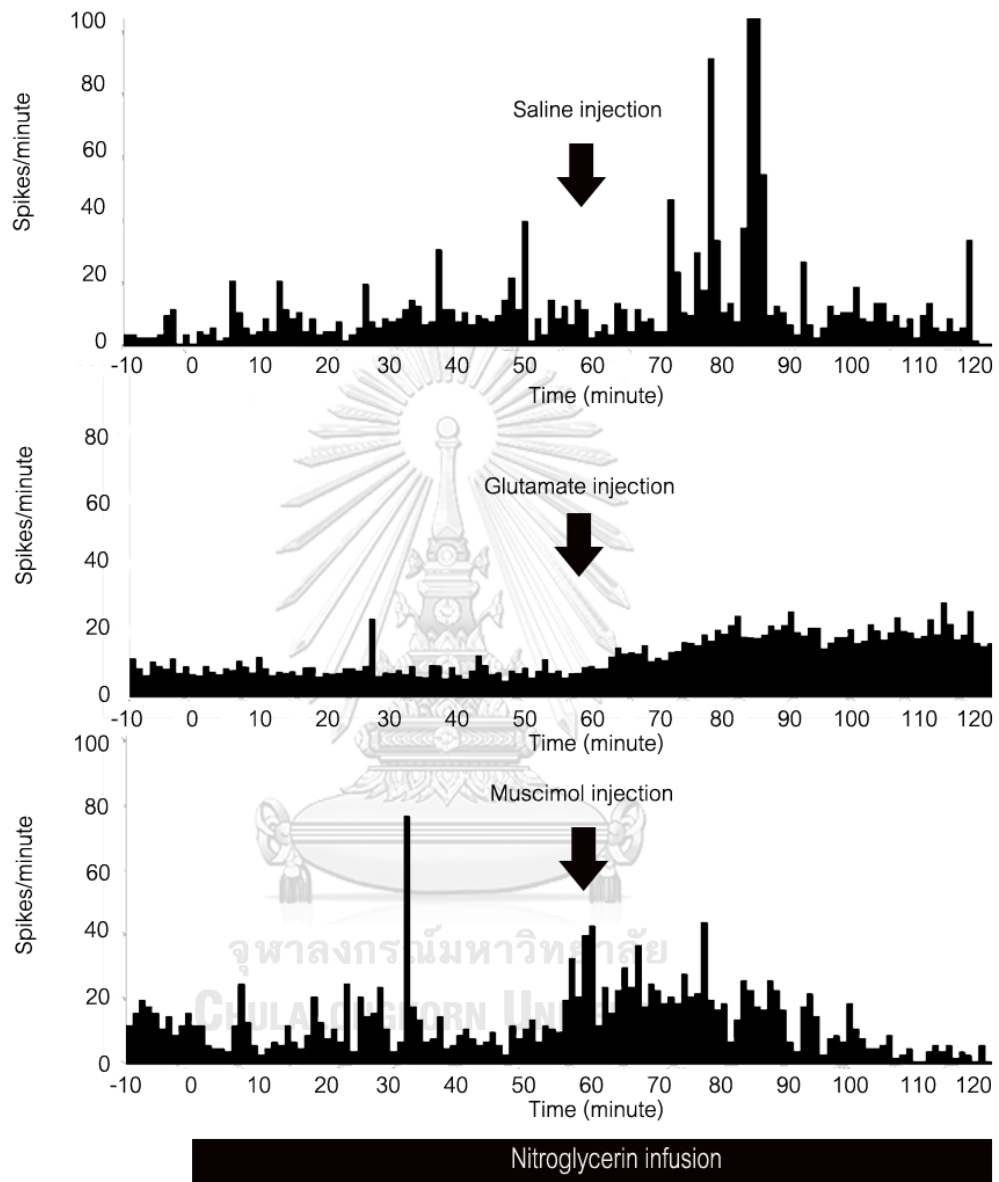


Figure 26 Effect of chronic paracetamol exposure and modulating effect of microninjection into nucleus raphe magnus on nitroglycerin-evoked neuronal firing in trigeminal nucleus caudalis (representative records of patterns of TNC firing).

In the paracetamol-treated rats, the number of TNC firing was not significantly different after glutamate or muscimol microinjection at NRM.

The extracellular signaling was shown in the percent of baseline value in 20 minutes interval after the onset of NTG infusion. Table 4 showed the NTG-induced TNC neuronal firing between control and paracetamol-treated groups in 60 minutes before NRM microinjection. An increase of neuronal excitability in both control and paracetamol-treated groups was found almost immediately after the onset of NTG infusion. TNC neuronal firing statistically increased within 20 minutes post-NTG infusion in control and paracetamol-treated groups (117.6 ± 22.7 percent, $P < 0.05$ and 117.8 ± 31.4 percent, $P = 0.013$ respectively). Though, the NTG-induced TNC neuronal firing in chronic paracetamol-treated rats was not significant different compared with control rats in 0-20, 20-40 and 40-60 minutes interval ($P = 0.537$, $P = 0.580$ and $P = 0.595$ respectively).

Table 4 The average of neuronal firing at trigeminal nucleus caudalis after nitroglycerin infusion

* $P < 0.05$ compared within group with baseline

The averages of TNC neuronal activity were shown in 20 minute interval after microinjection at NRM of control and paracetamol-treated groups (Table 5). In control groups, glutamate microinjection decreased the TNC firing. The numbers of TNC firing in the 20 minutes post-microinjection were 133.7 ± 31.1 and 182.1 ± 35.6 percent for glutamate and saline microinjection groups, respectively ($P = 0.009$). The percent of spikes at 40 minutes in the glutamate and saline microinjection groups were 109.1 ± 37.5 and 171.5 ± 21.7 percent, respectively ($P = 0.009$). At 60 minutes, the percent of TNC firing rates were 113.7 ± 56.9 and 158.9 ± 59.5 percent in the glutamate and saline microinjection groups, respectively ($P = 0.141$). On the other hand, muscimol microinjection was shown to increase the number of TNC firing compared with saline

microinjection in the control group. The TNC firing rates in muscimol microinjection group were 306.5 ± 107.3 , 289.2 ± 141.7 and 246.3 ± 105.2 percent at 20, 40 and 60 minutes, respectively ($P=0.005$, $P=0.046$ and $P=0.093$).

In the paracetamol-treated rats, the number of TNC firing was not significantly different after glutamate microinjection. The numbers of TNC firing in the 20 minutes post-microinjection were 174.8 ± 56.6 and 253.7 ± 67.2 percent for glutamate and saline microinjection groups, respectively ($P=0.064$). The percent of spikes at 40 minutes in the glutamate and saline microinjection groups were 181.8 ± 49.5 and 216.9 ± 18.5 percent, respectively ($P=0.132$). At 60 minutes, the percent of TNC firing rates were 178.9 ± 56.6 and 221.2 ± 36.1 percent in the glutamate and saline microinjection groups, respectively ($P=0.083$). Also, the TNC firing rate after muscimol microinjection did not show the statistical different from saline microinjection in paracetamol-treated group. The number of TNC firing in muscimol microinjection group were 306.5 ± 107.3 , 289.2 ± 141.7 and 246.3 ± 105.2 percent at 20, 40 and 60 minutes, respectively ($P=0.728$, $P=0.908$ and $P=0.563$). The effects of chronic paracetamol treatment and NRM microinjection on NTG-evoked TNC neuronal firing in 2 hours were demonstrated in Figure 27.

Table 5 The average of neuronal firing at trigeminal nucleus caudalis after nucleus raphe magnus microinjection

Neuronal firing (percent of baseline)	Control groups			Paracetamol-treated groups		
	Saline injection	Glutamate injection	Muscimol injection	Saline injection	Glutamate injection	Muscimol injection
0-20min	182.1 ± 35.6	$133.7 \pm 31.1^*$	$306.5 \pm 107.3^*$	$253.7 \pm 67.2^*$	174.8 ± 56.6	249.5 ± 96.4
20-40min	171.5 ± 21.7	$109.1 \pm 37.5^*$	$289.2 \pm 141.7^*$	$216.9 \pm 18.5^*$	181.8 ± 49.5	295.0 ± 157.7
40-60min	158.9 ± 59.5	113.7 ± 56.9	246.3 ± 105.2	221.2 ± 36.1	178.9 ± 56.6	232.4 ± 152.4



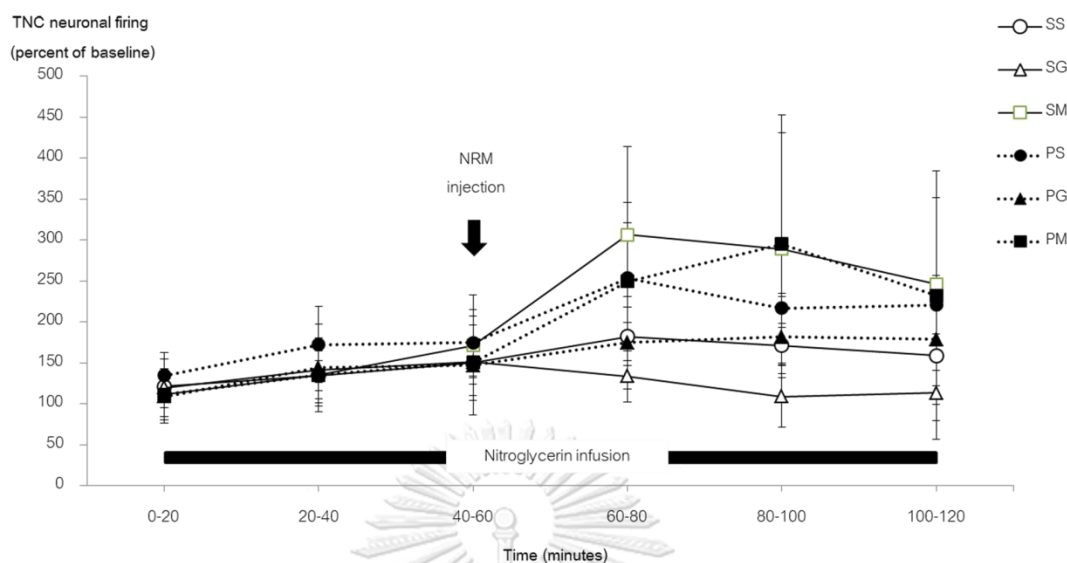


Figure 27 Effect of chronic paracetamol exposure and modulating effect of microinjection into nucleus raphe magnus on nitroglycerin-evoked neuronal firing in trigeminal nucleus caudalis.

In control groups, glutamate microinjection decreased the TNC firing whereas muscimol microinjection was shown to increase the number of TNC firing compared with saline microinjection. In contrast, the number of TNC firing of the paracetamol-treated groups was not significantly different after glutamate or muscimol microinjection at NRM. White circle with solid line, control group with saline microinjection; White triangle with solid line, control group with glutamate microinjection; White square with solid line, control group with muscimol microinjection; Black circle with dash line, paracetamol-treated group with saline microinjection; Black triangle with dash line, paracetamol-treated group with glutamate microinjection; Black square with dash line, paracetamol-treated group with muscimol microinjection

NTG-EVOKED FOS EXPRESSION

In primary somatosensory cortex, the numbers of Fos-IR cells were shown in Table 6 and Figure 28-29. The numbers of Fos-IR cells were counted at ipsilateral sides of meningeal stimulation. After chronic paracetamol treatment, Fos expression significantly increased compared with control group (Figure 28). The numbers of Fos-IR cells in the cortex seen in the paracetamol-treated and control groups with NRM saline-microinjection were 298.5 ± 169.6 and 104.1 ± 30.7 cells/mm², respectively ($P=0.050$).

Although, muscimol microinjection tended to increase the number of Fos-IR cells in control group, it did not significantly change the number of Fos-IR cells compared with saline microinjection. Also, glutamate microinjection did not alter the number of Fos-IR cells. The number of Fos-IR cells after glutamate and muscimol microinjection were 119.9 ± 56.8 and 189.0 ± 82.7 cells/ mm^2 , respectively ($P=0.564$ and $P=0.275$ respectively). Additionally, the number of Fos-IR cells did not change after NRM microinjection in paracetamol-treated group. The number of Fos-IR cells after glutamate microinjection was 280.5 ± 73.4 cells/ mm^2 , while the number of Fos-IR cells after muscimol microinjection was 258.6 ± 145.8 cells/ mm^2 ($P=0.827$ and $P=0.513$ respectively) (Figure 29).



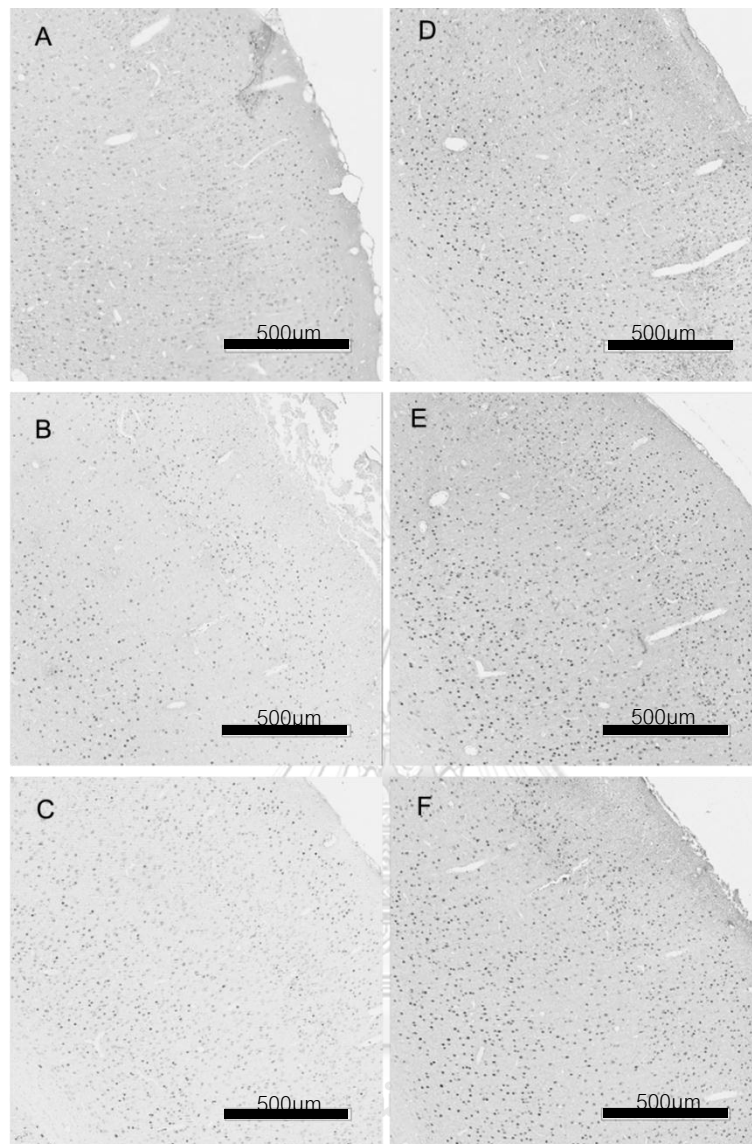


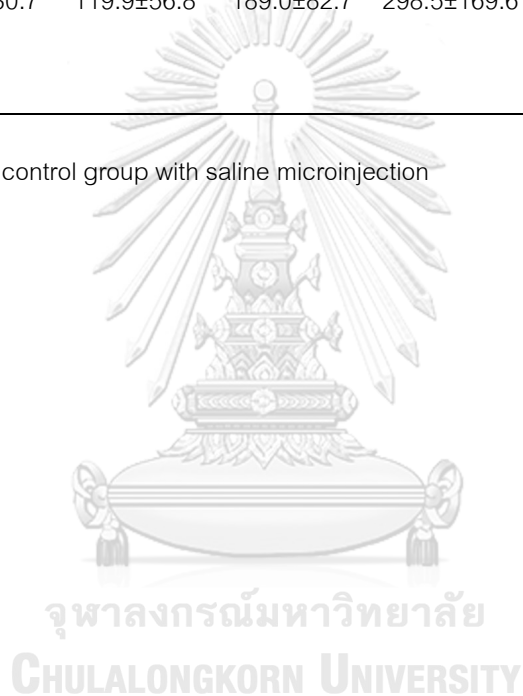
Figure 28 Photomicrograph shows the effects of chronic paracetamol exposure and modulating effect of microinjection into nucleus raphe magnus on nitroglycerin-evoked Fos expression at primary somatosensory cortex.

Chronic paracetamol exposure was shown to increase the number of NTG-evoked Fos expression in the ipsilateral cortex compared with control group. Glutamate or muscimol microinjection did not change the number of Fos-IR cells compared with saline microinjection in both control and paracetamol-treated groups. A: control with saline microinjection group. B: control with glutamate microinjection group. C: control with muscimol microinjection group. D: paracetamol-treated with saline microinjection group. E: paracetamol-treated with glutamate microinjection group. F: paracetamol-treated with muscimol microinjection group.

Table 6 The average numbers of nitroglycerin-evoked Fos expression in cortical neurons of primary somatosensory cortex

	Control groups			Paracetamol groups		
	Saline injection	Glutamate injection	Muscimol injection	Saline injection	Glutamate injection	Muscimol injection
Fos expression (cells/mm ²)	104.1±30.7	119.9±56.8	189.0±82.7	298.5±169.6*	280.5±73.4	258.6±145.8

* $P < 0.05$ compared to control group with saline microinjection



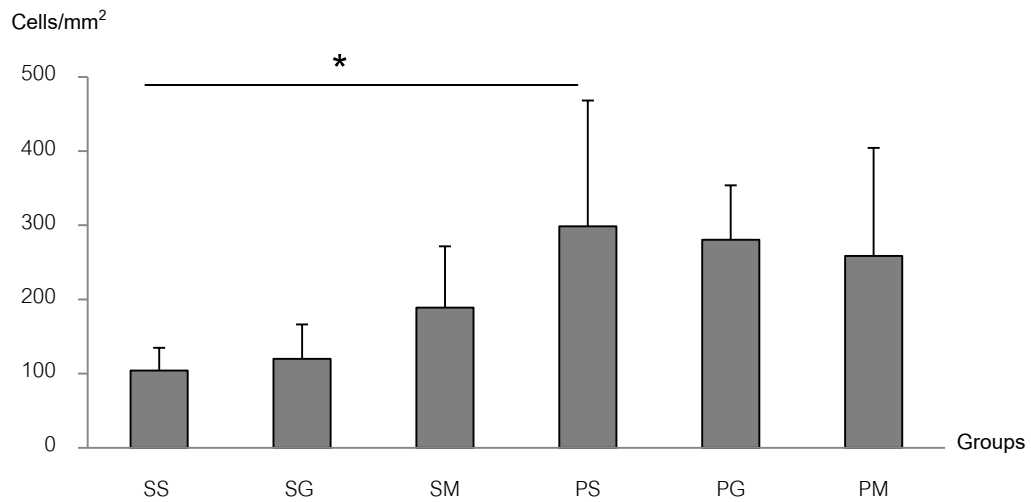
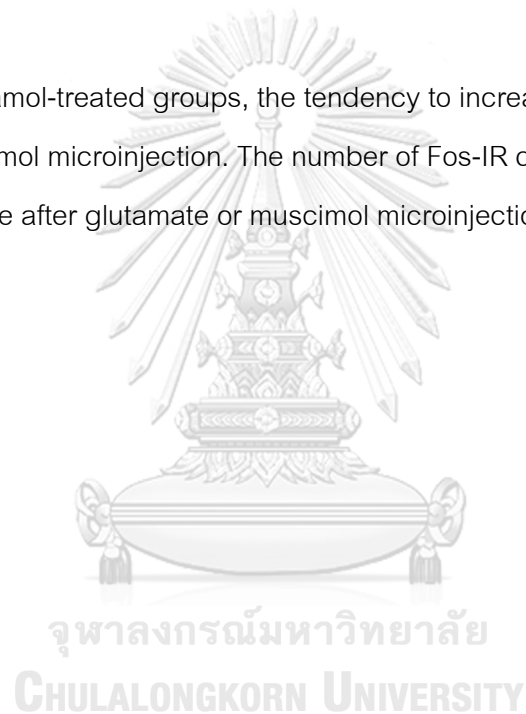


Figure 29 Effect of chronic paracetamol exposure and modulating effect of microninjection into nucleus raphe magnus on nitroglycerin-evoked Fos expression at primarysomatosensory cortex.

Chronic paracetamol exposure was shown to increase the number of NTG-evoked Fos expression in the ipsilateral cortex compared with control group. Glutamate or muscimol microinjection did not significantly change the number of Fos-IR cells compared with saline microinjection in both control and paracetamol-treated groups. $*P < 0.05$ compared ipsilateral side of CSD induction between groups. SS: control with saline microinjection group. SG: control with glutamate microinjection group. SM: control with muscimol microinjection group. PS: paracetamol-treated with saline microinjection group. PG: paracetamol-treated with glutamate microinjection group. PM: paracetamol-treated with muscimol microinjection group.

The numbers of Fos-IR cells in TNC were counted at ipsilateral sides of meningeal stimulation (Figure 30). Chronic paracetamol treatment increased the number of Fos-IR cells in the TNC compared with the control group (84.8 ± 29.1 and 49.9 ± 23.3 cells/slide respectively, $P=0.030$) (Table 7). In control group, glutamate microinjection at NRM did not significantly decrease the number of Fos-IR cells compared with saline microinjection (40.2 ± 11.8 and 49.9 ± 23.3 cells/slide respectively, $P=0.348$). Besides, the number of Fos-IR cells in TNC in the muscimol-treated group was 70.5 ± 25.1 cells/slide. Muscimol microinjection had a tendency to increase in the number of Fos-IR cells in the TNC ($P=0.110$).

In paracetamol-treated groups, the tendency to increase Fos expression was absent after muscimol microinjection. The number of Fos-IR cells in TNC did not significantly change after glutamate or muscimol microinjection at NRM (Figure 31).



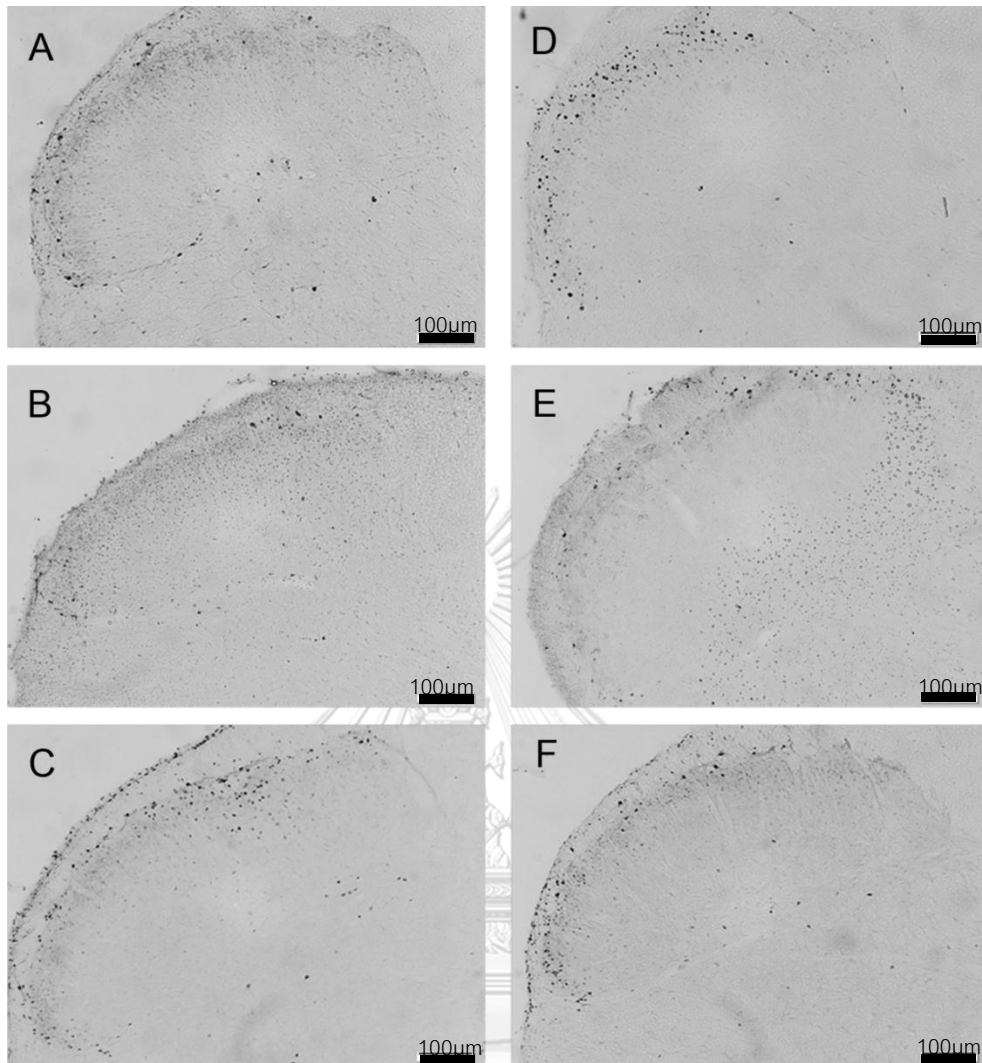


Figure 30 Photomicrograph shows the effects of chronic paracetamol exposure and modulating effect of microinjection into nucleus raphe magnus on nitroglycerin-evoked Fos expression at trigeminal nucleus caudalis.

Chronic paracetamol exposure was shown to increase the number of NTG-evoked Fos expression in the ipsilateral TNC compared with control group. Glutamate or muscimol microinjection did not significantly change the number of Fos-IR cells compared with saline microinjection in both control and paracetamol-treated groups. A: control with saline microinjection group. B: control with glutamate microinjection group. C: control with muscimol microinjection group. D: paracetamol-treated with saline microinjection group. E: paracetamol-treated with glutamate microinjection group. F: paracetamol-treated with muscimol microinjection group.

Table 7 The average numbers of nitroglycerin-evoked Fos expression in neurons of trigeminal nucleus caudalis

	Control groups			Paracetamol-treated groups		
	Saline injection	Glutamate injection	Muscimol injection	Saline injection	Glutamate injection	Muscimol injection
Fos expression (cells/slide)	49.9±23.3	40.2±11.8	70.5±25.1	84.8±29.1*	75.9±25.4	72.2±14.1

* $P < 0.05$ compared to control group with saline microinjection

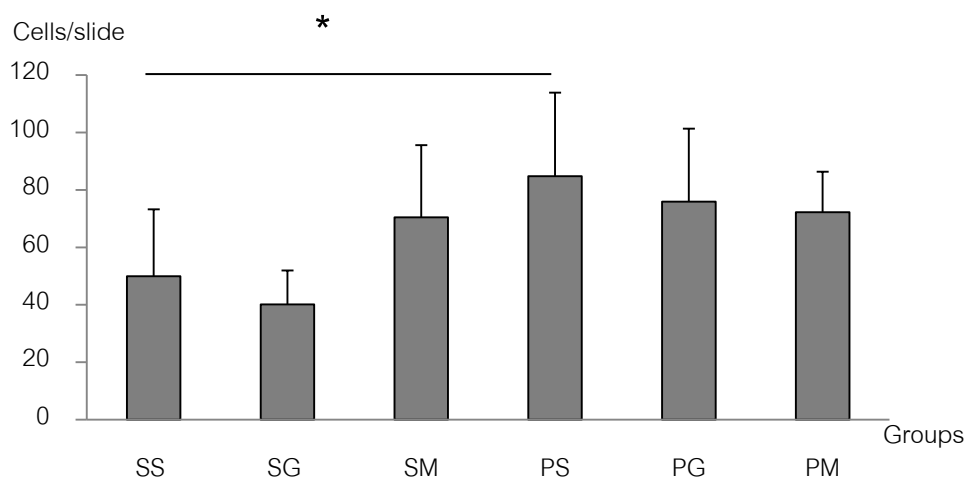


Figure 31 Effects of chronic paracetamol exposure and modulating effect of microninjection into nucleus raphe magnus on nitroglycerin-evoked Fos expression at trigeminal nucleus caudalis.

Chronic paracetamol exposure was shown to increase the number of NTG-evoked Fos expression in the ipsilateral TNC compared with control group. Glutamate or muscimol microinjection did not significantly change the number of Fos-IR cells compared with saline microinjection in both control and paracetamol-treated groups. * $P < 0.05$ compared ipsilateral side of CSD induction between groups. SS: control with saline microinjection group. SG: control with glutamate microinjection group. SM: control with muscimol microinjection group. PS: paracetamol-treated with saline microinjection group. PG: paracetamol-treated with glutamate microinjection group. PM: paracetamol-treated with muscimol microinjection group.

CHAPTER 5

DISCUSSION AND CONCLUSION

EFFECT OF CHRONIC PARACETAMOL EXPOSURE

In this study, chronic paracetamol administration was shown to increase the CSD susceptibility. Also, the increase of neuronal firing at TNC was found in NTG-infusion model after long term paracetamol treatment. It is consistent with the former study which showed that chronic paracetamol exposure increased CSD development and CSD-evoked Fos-IR cells in the TNC (12). Because of the hallmarks of CSD are the complete membrane depolarization of neurons and glia, an increase of the number of CSD wave represents the hyper-sensitization of cortical neurons. These finding suggest that chronic paracetamol exposure can increase the neuronal excitability of the cortex and TNC.

An increase of the neuronal excitability after chronic paracetamol treatment may a result from the major change of serotonergic system and the imbalance of amino acid in the brain structures. Serotonin-depleted rats were shown to enhance CSD-evoked cortical excitability and CSD-evoked TNC neuronal excitability (82). Additionally, chronic paracetamol administration resulted in the decrease of analgesic efficacy coincide with the decrease in platelet 5-HT level (9). Furthermore, Supornsilpchai and colleagues reported that chronic paracetamol exposure lead to an up-regulation of pro-nociceptive 5-HT_{2A} receptor in cerebral cortex and trigeminal ganglion which relate to cortical hyper-excitation and trigeminal nociceptive facilitation (10). The former studies from Blecharz and colleagues demonstrated that eight-week long subcutaneous paracetamol treatment results in the reduction of serotonergic neurotransmitter and the increase of GABA amino acid in the prefrontal cortex (76, 83).

Since paracetamol shows a low affinity to 5-HT receptors, an indirect action between paracetamol and serotonin system may a result from cannabinoid receptor activation. An active metabolite of paracetamol, AM404, was shown to indirectly activate cannabinoid receptor because of AM404 inhibits the degradation and reuptake of

anandamide, the endocannabinoid (75, 84). Therefore, chronic paracetamol treatment seems to prolong activate cannabinoid receptors, CB₁ and CB₂, which are found in the brain and brainstem (85). Based on these previous studies, long term cannabinoid receptors activation is one of the possible mechanisms which lead to an increase of neuronal excitability after chronic paracetamol treatment. The study from Tao R. and Ma Z. suggested that cannabinoids can exert effect on 5-HT efflux in the neural circuit between dorsal raphe nucleus and nucleus accumbens depending on the direct or indirect effect of CB₁ receptor (86). Moreover, Hill and colleagues examined the reciprocal interaction between 5-HT_{1A} and 5-HT_{2A} receptors after chronic cannabinoid administration by using behavioral, physiological and hormonal measurements. They reported that chronic cannabinoid treatment can up-regulate 5-HT_{2A} receptor activity, while concurrently down-regulate 5-HT_{1A} receptor activity (87).

Since the release of ions and neurotransmitters, especially K⁺, Ca²⁺ and glutamate, to the extracellular space is the important step to induce CSD propagation, an alteration of CSD susceptibility by 5-HT system may relate to the modulation of these factors. For instance, the 5-HT_{1A} and 5-HT_{1D} receptors activation was shown to inhibit N- and P/Q-type Ca²⁺ channels (88). This leads to the reduction of glutamate release (89).

INVOLVEMENT OF NRM ON THE CORTICAL EXCITABILITY

As mentioned above, the enhancing effect of chronic paracetamol exposure on neurons in cerebral cortex and central trigeminal nociceptive pathway may be the result of altered central serotonin-dependent modulation system. Therefore, in this study, direct microinjection with glutamate or muscimol was done into NRM, a major serotonin nucleus.

This study demonstrated that muscimol microinjection in non-treated animals exhibited the enhancement of CSD development and CSD-evoked Fos expression in cortex and TNC. Central serotonin function seems to disinhibit by direct microinjection with muscimol into NRM. It is consistent with the original hypothesis from Bausbaum and Fields in 1984. They proposed that GABAergic interneurons in the NRM tonically release GABA neurotransmitter which inhibits spinally projecting neurons via GABA_A receptors

activation (31). On the other hand, NRM stimulation by glutamate microinjection did not reduce the number of CSD wave and CSD-evoked FOS expression. This result may associate to the tonically release of serotonin from the serotonergic cells in NRM (90). Furthermore, Mason P. et al. suggested that serotonin indirectly modulate the nociceptive transmission by mediating neuropeptides and other neurotransmitters (90).

This study also showed that chronic analgesic exposure may alter the function of NRM. In the paracetamol-treated animals, microinjection with glutamate or muscimol neither changed the CSD development nor CSD-evoked FOS expression in cortex and TNC.

INVOLVEMENT OF NRM ON THE TRIGEMINAL NOCICEPTIVE SYSTEM

Based on the CSD model, it is not possible to conclude whether the facilitation of trigeminal nociception was caused by the direct effect upon trigeminal nociceptive system or indirectly via the increased CSD response. As we known that trigeminal ganglion and TNC were stimulated by CSD event (59, 60). To investigate this problem, NTG infusion model was used in this study to bypass the effect of CSD activation. The increased of TNC neuronal firing observed in NTG infusion model indicated that chronic paracetamol treatment can directly affect the trigeminal nociceptive system.

In the present study, muscimol microinjection in control rats can increase NTG-induced TNC neuronal firing, while glutamate microinjection was shown to decrease NTG-induced TNC neuronal firing. These findings are consistent with the previous studies which showed that GABA_A receptor agonist microinjection at NRM facilitated craniovascular nociceptive transmission (91). In addition, an activation of NRM by glutamate microinjection facilitates the descending inhibitory influence on the spinal nociceptive transmission (92, 93). In this study, direct microinjection with muscimol into NRM seems to inhibit central serotonin function by hyperpolarizing 5-HT neurons leading to facilitation of the spinal medullary transmission. In contrast, glutamate microinjection may activate serotonergic neurons resulting in descending inhibitory transmission at medullary dorsal horn. These results supported by the extensive evidences which demonstrated biphasic modulation, facilitation and inhibition, from

NRM to spinal medullary transmission. Though, not only serotonergic neurons but also GABAergic neurons, Glycinergic neurons and several neuropeptides were found in NRM (36, 94, 95). Accordingly, an absolute outcome came from a non-specific activation or inhibition of all NRM neurons. The present study demonstrated that TNC neuronal firing was significantly changed for forty minutes after NRM microinjection in control rats. However, there is not difference in the last twenty-minute period. Likewise, the number of Fos-IR cells did not significantly alter. The influence of continuous NTG infusion must be taken into account. The exogenous nitric oxide was shown to attenuate the descending inhibitory pain transmission (96). Furthermore, the increased FOS expression was found in the spinal dorsal horn after NO perfusion (97). Hence, the continuous NO infusion seems to maintain the neuronal activation. Moreover, the electrophysiological study from Fossier P. et al. reported the modification of 5-HT by NO (98). This study showed a decrease of 5-HT efficacy to modulate cholinergic synaptic transmission after NO application or nitric oxide synthase (NOS) activation.

The change of TNC neuronal firing observed in NTG infusion model after NRM microinjection confirmed a significant role of NRM in optimizing sensitivity of trigeminal nociceptive neurons. Consistent with CSD model, the alteration of NRM function was shown after chronic paracetamol treatment. Glutamate or muscimol microinjection at NRM did not change the NTG-induced trigeminal neuronal firing in the paracetamol-treated animals.

From the present study, NRM, the major serotonergic brainstem nucleus, was shown to modulate the neuronal excitability of central trigeminal nociceptive system. An alteration of NRM function was found after chronic paracetamol exposure. It can be concluded that the medication-induced NRM dysfunction is a possible mechanism underlying the pathogenesis of MOH.

REFERENCES

1. IHS. The international classification of headache disorders, 3rd edition (beta version). *Cephalalgia*. 2013;33(9):629-808.
2. Kristoffersen ES, Lundqvist C. Medication-overuse headache: epidemiology, diagnosis and treatment. *Therapeutic advances in drug safety*. 2014;5(2):87-99.
3. Okada-Ogawa A, Porreca F, Meng ID. Sustained morphine-induced sensitization and loss of diffuse noxious inhibitory controls in dura-sensitive medullary dorsal horn neurons. *The journal of neuroscience*. 2009;29(50):15828-35.
4. Gardell LR, Wang R, Burgess SE, Ossipov MH, Vanderah TW, Malan TP, et al. Sustained morphine exposure induces a spinal dynorphin-dependent enhancement of excitatory transmitter release from primary afferent fibers. *The journal of neuroscience*. 2002;22(15):6747-55.
5. De Felice M, Ossipov MH, Wang R, Lai J, Chichorro J, Meng I, et al. Triptan-induced latent sensitization: A possible basis for medication overuse headache. *Annals of neurology*. 2010;67(3):325-37.
6. Coppola G, Currà A, Di Lorenzo C, Parisi V, Gorini M, Sava SL, et al. Abnormal cortical responses to somatosensory stimulation in medication-overuse headache. *BMC neurology*. 2010;10(1):126-34.
7. Srikiatkachorn A, le Grand SM, Supornsilpchai W, Storer RJ. Pathophysiology of medication overuse headache—an update. *Headache: the journal of head and face pain*. 2013;54(1):204-10.
8. Richerson GB, Aston-Jones G, Saper CB. The modulatory function of the brain stem. In: Kandel ER, editor. *Principles of neural science*. 5 ed. USA: McGraw-Hill companies; 2013. p. 1038-55.
9. Srikiatkachorn A, Tarasub N, Govitrapong P. Effect of chronic analgesic exposure on the central serotonin system: a possible mechanism of analgesic abuse headache. *Headache: the journal of head and face pain*. 2000;40(5):343-50.
10. Supornsilpchai W, le Grand SM, Srikiatkachorn A. Involvement of pro-nociceptive 5-

HT2A receptor in the pathogenesis of medication-overuse headache. *Headache: the journal of head and face pain*. 2010;50(2):185-97.

11. Su M, Ran Y, Han X, Liu Y, Zhang X, Tan Q, et al. Rizatriptan overuse promotes hyperalgesia induced by dural inflammatory stimulation in rats by modulation of the serotonin system. *European journal of neuroscience*. 2016;44(4):2129-38.

12. Supornsilpchai W, le Grand SM, Srikiatkachorn A. Cortical hyperexcitability and mechanism of medication-overuse headache. *Cephalalgia*. 2010;30(9):1101-9.

13. Ayzenberg I, Obermann M, Nyhuis P, Gastpar M, Limmroth V, Diener HC, et al. Central sensitization of the trigeminal and somatic nociceptive systems in medication overuse headache mainly involves cerebral supraspinal structures. *Cephalalgia*. 2006;26(9):1106-14.

14. Currà A, Coppola G, Gorini M, Porretta E, Bracaglia M, Di Lorenzo C, et al. Drug-induced changes in cortical inhibition in medication overuse headache. *Cephalalgia*. 2011;31(12):1282-90.

15. Srikiatkachorn A, Anthony M. Serotonin receptor adaptation in patients with analgesic-induced headache. *Cephalalgia*. 1996;16(6):419-22.

16. Srikiatkachorn A, Anthony M. Platelet serotonin in patients with analgesic-induced headache. *Cephalalgia*. 1996;16(6):423-6.

17. Srikiatkachorn A, Puangniyom S, Govitrapong P. Plasticity of 5-HT_{2A} Serotonin Receptor in Patients With Analgesic-Induced Transformed Migraine. *Headache: the journal of head and face pain*. 1998;38(7):534-9.

18. Ma W, Zheng W-H, Kar S, Quirion R. Morphine treatment induced calcitonin gene-related peptide and substance P increases in cultured dorsal root ganglion neurons. *Neuroscience*. 2000;99(3):529-39.

19. Yokota C, Kuge Y, Hasegawa Y, Tagaya M, Abumiya T, Ejima N, et al. Unique profile of spreading depression in a primate model. *Journal of cerebral blood flow and metabolism*. 2002;22(7):835-42.

20. Trang T, Quirion R, Jhamandas K. The spinal basis of opioid tolerance and physical dependence: Involvement of calcitonin gene-related peptide, substance P, and

arachidonic acid-derived metabolites. *Peptides*. 2005;26(8):1346-55.

21. Vibulyaseck S, Bongsebandhu-phubhakdi S, Grand SMI, Srikiatkachorn A. Potential risk of dihydroergotamine causing medication overuse headache: preclinical evidence. *Asian biomedicine*. 2014;8:323-31.
22. Perrotta A, Serrao M, Sandrini G, Burstein R, Sances G, Rossi P, et al. Sensitisation of spinal cord pain processing in medication overuse headache involves supraspinal pain control. *Cephalalgia*. 2009;30(3):272-84.
23. Riederer F, Marti M, Luechinger R, Lanzenberger R, von Meyenburg J, Gantenbein AR, et al. Grey matter changes associated with medication-overuse headache: correlations with disease related disability and anxiety. *The world journal of biological psychiatry*. 2012;13(7):517-25.
24. Riederer F, Gantenbein AR, Marti M, Luechinger R, Kollias S, Sándor PS. Decrease of gray matter volume in the midbrain is associated with treatment response in medication-overuse headache: possible influence of orbitofrontal cortex. *The journal of neuroscience*. 2013;33(39):15343-9.
25. Meng ID, Harasawa I. Chronic morphine exposure increases the proportion of on-cells in the rostral ventromedial medulla in rats. *Life sciences*. 2007;80(20):1915-20.
26. Vanderah TW, Suenaga NM, Ossipov MH, Malan TP, Lai J, Porreca F. Tonic descending facilitation from the rostral ventromedial medulla mediates opioid-induced abnormal pain and antinociceptive tolerance. *The journal of neuroscience*. 2001;21(1):279-86.
27. Dubner R, Bennett GJ. Spinal and trigeminal mechanisms of nociception. *Annual review of neuroscience*. 1983;6(1):381-418.
28. Goadsby PJ. Pathophysiology of migraine. *Neurologic clinics*. 2009;27(2):335-60.
29. May A, Goadsby PJ. The trigeminovascular system in humans: pathophysiologic implications for primary headache syndromes of the neural influences on the cerebral circulation. *Journal of cerebral blood flow and metabolism* 1999;19(2):115-27.
30. Ossipov MH, Dussor GO, Porreca F. Central modulation of pain. *The journal of clinical investigation*. 2010;120(11):3779-87.

31. Basbaum AI, Fields HL. Endogenous pain control systems: brainstem spinal pathways and endorphin circuitry. *Annual review of neuroscience*. 1984;7:309-38.
32. Paxinos G, Watson C. *The rat brain in stereotaxic coordinates*. 2 ed. Sydney: Harcourt Brace Jovanovich; 1986.
33. Bowker RM. The relationship between descending serotonin projections and ascending projections in the nucleus raphe magnus: a double labeling study. *Neuroscience letters*. 1986;70(3):348-53.
34. Lambert G, Hoskin K, Zagami A. Cortico-NRM Influences on Trigeminal Neuronal Sensation. *Cephalalgia*. 2008;28(6):640-52.
35. Zhuo M, Gebhart G. Biphasic modulation of spinal nociceptive transmission from the medullary raphe nuclei in the rat. *Journal of neurophysiology*. 1997;78(2):746-58.
36. Hornung J-P. Raphe Nuclei A2. In: Mai JK, Paxinos G, editors. *The Human Nervous System*. 3 ed. San Diego: Academic Press; 2012. p. 401-24.
37. Goadsby PJ, Lipton RB, Ferrari MD. Migraine — Current Understanding and Treatment. *The New England journal of medicine*. 2002;346(4):257-70.
38. Andreou AP, Summ O, Charbit AR, Romero-Reyes M, Goadsby PJ. Animal models of headache: from bedside to bench and back to bedside. *Expert reviews of neurotherapeutics*. 2010;10(3):389-411.
39. Olesen J, Iversen HK, Thomsen LL. Nitric oxide supersensitivity: a possible molecular mechanism of migraine pain. *Neuroreport*. 1993;4(8):1027-30.
40. Iversen HK, Olesen J, Tfelt-Hansen P. Intravenous nitroglycerin as an experimental model of vascular headache. Basic characteristics. *Pain*. 1989;38(1):17-24.
41. Tfelt-Hansen PC, Tfelt-Hansen J. Nitroglycerin headache and nitroglycerin-induced primary headaches from 1846 and onwards: a historical overview and an update. *Headache: the journal of head and face pain*. 2009;49(3):445-56.
42. Afridi SK, Kaube H, Goadsby PJ. Glyceryl trinitrate triggers premonitory symptoms in migraineurs. *Pain*. 2004;110(3):675-80.
43. Bates EA, Nikai T, Brennan KC, Fu YH, Charles AC, Basbaum AI, et al. Sumatriptan alleviates nitroglycerin-induced mechanical and thermal allodynia in mice. *Cephalalgia*.

2010;30(2):170-8.

44. Bergerot A, Holland P, Akerman S, Bartsch T, Ahn A, MaassenVanDenBrink A, et al. Animal models of migraine: looking at the component parts of a complex disorder. *European journal of neuroscience*. 2006;24(6):1517-34.

45. Pradhan AA, Smith ML, McGuire B, Tarash I, Evans CJ, Charles A. Characterization of a novel model of chronic migraine. *Pain*. 2014;155(2):269-74.

46. Lassen LH, Ashina M, Christiansen I, Ulrich V, Olesen J. Nitric oxide synthase inhibition in migraine. *The lancet*. 1997;349(9049):401-2.

47. Koulchitsky S, Fischer MJ, Messlinger K. Calcitonin gene-related peptide receptor inhibition reduces neuronal activity induced by prolonged increase in nitric oxide in the rat spinal trigeminal nucleus. *Cephalalgia*. 2009;29(4):408-17.

48. Tassorelli C, Joseph SA. Systemic nitroglycerin induces Fos immunoreactivity in brainstem and forebrain structures of the rat. *Brain research*. 1995;682(1-2):167-81.

49. Moncada S, Palmer RM, Higgs EA. Nitric oxide: physiology, pathophysiology, and pharmacology. *Pharmacological reviews*. 1991;43(2):109-42.

50. Kruuse C, Thomsen LL, Jacobsen TB, Olesen J. The phosphodiesterase 5 inhibitor sildenafil has no effect on cerebral blood flow or blood velocity, but nevertheless induces headache in healthy subjects. *Journal of cerebral blood flow and metabolism*. 2002;22(9):1124-31.

51. Kruuse C, Thomsen LL, Birk S, Olesen J. Migraine can be induced by sildenafil without changes in middle cerebral artery diameter. *Brain*. 2003;126(1):241-7.

52. Gozalov A, Jansen-Olesen I, Klaerke D, Olesen J. Role of BKCa channels in cephalic vasodilation induced by CGRP, NO and transcranial electrical stimulation in the rat. *Cephalalgia*. 2007;27(10):1120-7.

53. Reuter U, Bolay H, Jansen-Olesen I, Chiarugi A, Sanchez del Rio M, Letourneau R, et al. Delayed inflammation in rat meninges: implications for migraine pathophysiology. *Brain*. 2001;124(12):2490-502.

54. Messlinger K, Lennerz JK, Eberhardt M, Fischer MJ. CGRP and NO in the trigeminal system: mechanisms and role in headache generation. *Headache: the journal of head and*

face pain. 2012;52(9):1411-27.

55. Bagdy G, Riba P, Kecskeméti V, Chase D, Juhász G. Headache-type adverse effects of NO donors: vasodilation and beyond. *British journal of pharmacology*. 2010;160(1):20-35.

56. Ferrari LF, Levine JD, Green PG. Mechanisms mediating nitroglycerin-induced delayed-onset hyperalgesia in the rat. *Neuroscience*. 2016;317(Supplement C):121-9.

57. Cutrer FM, Black DF. Imaging Findings of Migraine. *Headache: the journal of head and face pain*. 2006;46(7):1095-107.

58. Gorji A, Speckmann EJ. Spreading depression enhances the spontaneous epileptiform activity in human neocortical tissues. *European journal of neuroscience*. 2004;19(12):3371-4.

59. Zhang X, Levy D, Kainz V, Nosedá R, Jakubowski M, Burstein R. Activation of central trigeminovascular neurons by cortical spreading depression. *Annals of neurology*. 2011;69(5):855-65.

60. Zhang X, Levy D, Nosedá R, Kainz V, Jakubowski M, Burstein R. Activation of meningeal nociceptors by cortical spreading depression: implications for migraine with aura. *The journal of neuroscience*. 2010;30(26):8807-14.

61. Leo AAP. Spreading depression of activity in the cerebral cortex. *Journal of neurophysiology*. 1944;7(6):359-90.

62. Eikermann-Haerter K, Ayata C. Cortical spreading depression and migraine. *Current neurology and neuroscience reports*. 2010;10(3):167-73.

63. Green AL, Gu P, De Felice M, Dodick D, Ossipov MH, Porreca F. Increased susceptibility to cortical spreading depression in an animal model of medication-overuse headache. *Cephalalgia*. 2013;34(8):594-604.

64. Morgan JI, Curran T. Role of ion flux in the control of c-fos expression. *Nature*. 1986;322(6079):552-5.

65. Morgan J, Cohen D, Hempstead J, Curran T. Mapping patterns of c-fos expression in the central nervous system after seizure. *Science*. 1987;237(4811):192-7.

66. Bullitt E. Expression of C-fos-like protein as a marker for neuronal activity following

- noxious stimulation in the rat. *Journal of comparative neurology*. 1990;296(4):517-30.
67. Hunt SP, Pini A, Evan G. Induction of c-fos-like protein in spinal cord neurons following sensory stimulation. *Nature*. 1987;328(6131):632-4.
68. Rowlinson SW, Kiefer JR, Prusakiewicz JJ, Pawlitz JL, Kozak KR, Kalgutkar AS, et al. A novel mechanism of cyclooxygenase-2 inhibition involving interactions with Ser-530 and Tyr-385. *Journal of biological chemistry*. 2003;278(46):45763-9.
69. Smith WL, DeWitt DL, Garavito RM. Cyclooxygenases: structural, cellular, and molecular biology. *Annual review of biochemistry*. 2000;69:145-82.
70. Aronoff DM, Oates JA, Boutaud O. New insights into the mechanism of action of acetaminophen: Its clinical pharmacologic characteristics reflect its inhibition of the two prostaglandin H₂ synthases. *Clinical pharmacology and therapeutics*. 2006;79(1):9-19.
71. Pickering G, Lorient MA, Libert F, Eschali r A, Beaune P, Dubray C. Analgesic effect of acetaminophen in humans: first evidence of a central serotonergic mechanism. *Clinical pharmacology and therapeutics*. 2006;79(4):371-8.
72. Bhosale UA, Khobragade R, Naik C, Yegnanarayan R, Kale J. Postoperative pharmacodynamic interaction of ondansetron; a 5-HT₃ antagonist and paracetamol in patients operated in the ENT department under local anesthesia. *Journal of basic and clinical pharmacy*. 2014;5(3):84.
73. Tjolsen A, Lund A, Hole K. Antinociceptive effect of paracetamol in rats is partly dependent on spinal serotonergic systems. *European journal of pharmacology*. 1991;193(2):193-201.
74. Sandrini M, Vitale G, Ruggieri V, Pini LA. Effect of acute and repeated administration of paracetamol on opioidergic and serotonergic systems in rats. *Inflammation research*. 2007;56(4):139-42.
75. Hogestatt ED, Jonsson BA, Ermund A, Andersson DA, Bjork H, Alexander JP, et al. Conversion of acetaminophen to the bioactive N-acylphenolamine AM404 via fatty acid amide hydrolase-dependent arachidonic acid conjugation in the nervous system. *Journal of biological chemistry*. 2005;280(36):31405-12.
76. Blecharz-Klin K, Piechal A, Pyrzanowska J, Joniec-Maciejak I, Kiliszek P, Widy-

- Tyszkiewicz E. Paracetamol--the outcome on neurotransmission and spatial learning in rats. *Behavioural brain research*. 2013;253:157-64.
77. Blecharz-Klin K, Joniec-Maciejak I, Jawna K, Pyrzanowska J, Piechal A, Wawer A, et al. Developmental exposure to paracetamol causes biochemical alterations in medulla oblongata. *Environmental toxicology and pharmacology*. 2015;40(2):369-74.
78. Corcoran GB, Mitchell JR, Vaishnav YN, Horning EC. Evidence that acetaminophen and N-hydroxyacetaminophen form a common arylating intermediate, N-acetyl-p-benzoquinoneimine. *Molecular pharmacology*. 1980;18(3):536-42.
79. Ghanem CI, Pérez MJ, Manautou JE, Mottino AD. Acetaminophen from liver to brain: New insights into drug pharmacological action and toxicity. *Pharmacological research*. 2016;109:119-31.
80. Yisarakun W, Supornsilpchai W, Chantong C, Srikiatkachorn A, Maneesri-le Grand S. Chronic paracetamol treatment increases alterations in cerebral vessels in cortical spreading depression model. *Microvascular Research*. 2014;94(0):36-46.
81. Paxinos G, Watson C. *The rat brain in stereotaxic coordinates*. 2 ed. Sydney: Harcourt Brace Jovanovich; 1986. 474 p.
82. Supornsilpchai W, Sanguanrangsirikul S, Maneesri S, Srikiatkachorn A. Serotonin Depletion, Cortical Spreading Depression, and Trigeminal Nociception. *Headache: the journal of head and face pain*. 2006;46(1):34-9.
83. Blecharz-Klin K, Joniec-Maciejak I, Piechal A, Pyrzanowska J, Wawer A, Widy-Tyszkiewicz E. Paracetamol impairs the profile of amino acids in the rat brain. *Environmental toxicology and pharmacology*. 2014;37(1):95-102.
84. Mallet C, Eschalié A, Daulhac L. Paracetamol: Update on its Analgesic Mechanism of Action. In: Maldonado C, editor. *Pain Relief-From Analgesics to Alternative Therapies*: InTech; 2017. p. 207-24.
85. Zou S, Kumar U. Cannabinoid receptors and the endocannabinoid system: signaling and function in the central nervous system. *International journal of molecular sciences*. 2018;19(3):833-55.
86. Tao R, Ma Z. Neural circuit in the dorsal raphe nucleus responsible for cannabinoid-

mediated increases in 5-HT efflux in the nucleus accumbens of the rat brain. International scholarly research network pharmacology. 2012;2012:1-10.

87. Hill MN, Sun JC, Tse MT, Gorzalka BB. Altered responsiveness of serotonin receptor subtypes following long-term cannabinoid treatment. International journal of neuropsychopharmacology. 2006;9(3):277-86.

88. Sun QQ, Dale N. Differential inhibition of N and P/Q Ca^{2+} currents by 5-HT_{1A} and 5-HT_{1D} receptors in spinal neurons of *Xenopus* larvae. The journal of physiology. 1998;510(1):103-20.

89. Schmitz D, Empson RM, Heinemann U. Serotonin and 8-OH-DPAT reduce excitatory transmission in rat hippocampal area CA1 via reduction in presumed presynaptic Ca^{2+} entry. Brain research. 1995;701(1-2):249-54.

90. Mason P, Gao K. Raphe magnus serotonergic neurons tonically modulate nociceptive transmission. Pain forum. 1998;7(3):143-50.

91. Suprongsinchai W, Storer R, Hoffmann J, Andreou A, Akerman S, Goadsby P. GABA_A receptors in the nucleus raphe magnus modulate firing of neurons in the trigeminocervical complex. The journal of headache and pain. 2013;14(1):1.

92. McGowan MK, Hammond DL. Antinociception produced by microinjection of glutamate into the ventromedial medulla of the rat: mediation by spinal GABA_A receptors. Brain Research. 1993;620(1):86-96.

93. Aimone LD, Gebhart GF. Stimulation-produced spinal inhibition from the midbrain in the rat is mediated by an excitatory amino acid neurotransmitter in the medial medulla. The journal of neuroscience. 1986;6(6):1803-13.

94. Inyushkin A, Merkulova N, Orlova A, Inyushkina E. Local GABAergic modulation of the activity of serotonergic neurons in the nucleus raphe magnus. Neuroscience and behavioral physiology. 2010;40(8):885-93.

95. Polak JM. Neuropeptides in the CNS. Trends in neurosciences. 1991;14(12):533-4.

96. Lin Q, Wu J, Peng YB, Cui M, Willis WD. Nitric oxide-mediated spinal disinhibition contributes to the sensitization of primate spinothalamic tract neurons. Journal of neurophysiology. 1999;81(3):1086-94.

97. Wu J, Fang L, Lin Q, Willis WD. Fos expression is induced by increased nitric oxide release in rat spinal cord dorsal horn. *Neuroscience*. 2000;96(2):351-7.
98. Fossier P, Blanchard B, Ducrocq C, Leprince C, Tauc L, Baux G. Nitric oxide transforms serotonin into an inactive form and this affects neuromodulation. *Neuroscience*. 1999;93(2):597-603.



VITA

NAME Prangtip Potewiratnanond

DATE OF BIRTH 9 February 1982

PLACE OF BIRTH Bangkok

INSTITUTIONS ATTENDED 2008-2011 Master of Sciences (M.Sc.) in Occlusion,
Faculty of Dentistry, Chulalongkorn University, Thailand
2000-2006 Doctor of Dental Surgery (D.D.S.) with the
second class of honor, Faculty of Dentistry, Chulalongkorn
University, Thailand

HOME ADDRESS 7/228 Charnsamut village Bangmuang Muang
Samutprakarn 10270